Nils Kavermann

Benchmarking of a battery loader and its impact on the Garpenberg mine

Benchmarking of a battery loader and its impact on the Garpenberg mine

---

Master Thesis

By

Nils Lukas Kavermann M.Sc.

Matr.-Nr.: 414913

Study: European Mining, Minerals and Environmental Programm, M.Sc.

Advisor: Dennis Wagner M.Sc. Douwe Osinga M.Sc.

Supervisor: Univ.-Prof. Dr.-Ing. Elisabeth Clausen, Dr.-Ing. Amir Kianfar

Written at the Institute for Advanced Mining Technologies at

RWTH Aachen

Aachen, 13.09.2023

Zentrales Prüfungsamt/Central Examination Office

Statutory Declaration in Lieu of an Oath
Eidesstattliche Erklärung

Kavermann Nils

Name, Vorname/Last Name, First Name

Matrikelnummer (freiwillige Angabe)
Matriculation No. (optional)

Ich versichere hiermit an Eides Statt, dass ich die vorliegende Arbeit/Bachelorarbeit/ Masterarbeit* mit dem Titel

I hereby declare in lieu of an oath that I have completed the present paper/Bachelor thesis/Master thesis* entitled

Benchmarking of a battery loader and its impact on the Garpenberg mine

selbstständig und ohne unzulässige fremde Hilfe (insbes. akademisches Ghostwriting) erbracht habe. Ich habe keine anderen als die angegebenen Quellen und Hilfsmittel benutzt. Für den Fall, dass die Arbeit zusätzlich auf einem Datenträger eingereicht wird, erkläre ich, dass die schriftliche und die elektronische Form vollständig übereinstimmen. Die Arbeit hat in gleicher oder ähnlicher Form noch keiner Prüfungsbehörde vorgelegen.

independently and without illegitimate assistance from third parties (such as academic ghostwriters). I have used no other than the specified sources and aids. In case that the thesis is additionally submitted in an electronic format, I declare that the written and electronic versions are fully identical. The thesis has not been submitted to any examination body in this, or similar, form.

Ort, Datum/City, Date

Unterschrift/Signature

*Nichtzutreffendes bitte streichen

*Please delete as appropriate

Belehrung:
Official Notification:

§ 156 StGB: Falsche Versicherung an Eides Statt
Wer vor einer zur Abnahme einer Versicherung an Eides Statt zuständigen Behörde eine solche Versicherung falsch abgibt oder unter Berufung auf eine solche Versicherung falsch aussagt, wird mit Freiheitsstrafe bis zu drei Jahren oder mit Geldstrafe bestraft.

Para. 156 StGB (German Criminal Code): False Statutory Declarations
Whoever before a public authority competent to administer statutory declarations falsely makes such a declaration or falsely testifies while referring to such a declaration shall be liable to imprisonment not exceeding three years or a fine.

§ 161 StGB: Fahrlässiger Falscheid; fahrlässige falsche Versicherung an Eides Statt
(1) Wenn eine der in den §§ 154 bis 156 bezeichneten Handlungen aus Fahrlässigkeit begangen worden ist, so tritt Freiheitsstrafe bis zu einem Jahr oder Geldstrafe ein.
(2) Straflosigkeit tritt ein, wenn der Täter die falsche Angabe rechtzeitig berichtigt. Die Vorschriften des § 158 Abs. 2 und 3 gelten entsprechend.

Para. 161 StGB (German Criminal Code): False Statutory Declarations Due to Negligence
(1) If a person commits one of the offences listed in sections 154 through 156 negligently the penalty shall be imprisonment not exceeding one year or a fine.
(2) The offender shall be exempt from liability if he or she corrects their false testimony in time. The provisions of section 158 (2) and (3) shall apply accordingly.

Die vorstehende Belehrung habe ich zur Kenntnis genommen:
I have read and understood the above official notification:

Ort, Datum/City, Date

Unterschrift/Signature

Table of Content

List of Figures

List of Tables

List of Abbreviations

Symbol	Description
LHD	Load haul and dump truck
BLHD	Battery load haul and dump truck
LiFeP	Lithium-Iron-Phosphate
AI	Artificial Intelegient
NDA	Non-disclosure agreement
WC	Work cycle
WCT	Work cycle time
VPC	Vehicle production calculator
DPM	Diesel particulate matter
SOC	State of charge
EBIT	Earnings Before Interest and Taxes
CAPEX	Capital Expenditure
OPEX	Operating Expenditure
S-WC	Short-distance work cycle
L-WC	Long-distance work cycle
RE-WC	Remuck bay work cycle
AB-WC	Automate Bucket Fill work cycle
LCB	Deeper located charging bay to the operating face
HCB	Higher located charging bay to the operating face
EVs	Electric vehicles
ICE	Internal combustion engine

List of Formulas

Symbol	Unit	Description
A	%	Availability of mining equipment
UoA	%	Utilization of availability of mining equipment
MTBF	h	Mean Time Between Failure of Mobile Mining Equipment
MTTR	h	Mean Time To Repair of Mobile Mining Equipment
WTC	min	Time for one work cycle
WC speed	km/h	Average speed for each work cycle
BFF	t	Bucket Fill Factor: average load per bucket
P		Performance rate indicator (0-1)
OEE		Overall Equipment Efficiency factor (0-1)
NE	kWh/t	Energy usage per ton moved
Cost per ton	SEK/t	Cost calculation per machine per ton moved

Acknowledgements

I would like to express my gratitude to the individuals and organizations that played a crucial role in the completion of my thesis:

First, I would like to express my sincere gratitude to Douwe Osinga, Boliden's project manager, for the opportunity to collaborate with Boliden on this work. I am deeply grateful for the time, effort, invaluable guidance and unwavering confidence you have shown me throughout this endeavor.

I would also like to express my sincere gratitude to Dennis Wagner, PhD student at ATM RWTH Aachen, for his invaluable support, inspiration, and wise advice. Your scientific mentorship and generous time have been of great importance to my academic journey.

In addition, my sincere gratitude goes to all the dedicated employees of Boliden who generously gave their time and expertise, contributing significantly to the success of my work. Without their support and wealth of experience, achieving the present results would have been an insurmountable task.

I would like to pay special tribute to Jolanthe de Meyer, Cameron Crest, and Eric Östberg, who are members of the Sandvik team. Their invaluable support has been critical, especially in ensuring access to key simulation software and providing the necessary information to accurately evaluate the performance of the battery loader.

Last but not least, I would like to express my deep gratitude to my family and friends for their unwavering moral support and belief in my abilities. Their encouragement has been a major source of motivation during this academic journey.

1. Introduction

The mining industry has undergone three major industrial revolutions, with the fourth currently underway. The previous revolutions involved the discovery of coal and steam engine technology, the introduction of electrification, steel, and oil, and computer technology and digitisation. All of those discoveries and technologies led to an increase in production and productivity in the mining sector. However, modern mining faces challenges such as decreasing deposit grades, increasing waste volumes and costs, and the need to reduce carbon emissions due to climate change (Humphreys, 2020). These challenges can be mitigated through the fourth revolution, which involves automation, AI, and new environmental approaches like battery technology (Humphreys, 2020). The European Union's Green Deal aims to achieve carbon neutrality by 2050, posing significant challenges for industries like mining that consume vast amounts of energy, much of it derived from diesel engines. The mining industry's carbon footprint currently accounts for 4-7% of global greenhouse gas emissions (Hertwich, 2010). As a result, mining companies such as Boliden must act quickly to introduce carbon-free or carbon-neutral technologies to meet government regulations, investor expectations, and social demands. (Boliden Annual and Sustainability Report 2022)

A primary challenge in decarbonising mining operations is replacing diesel-powered mobile equipment such as Load and Dump (LHD) trucks and load trucks with electric alternatives. These vehicles are responsible for 15-20% of total operating costs in underground mining, with diesel fuel costs accounting for 13-16% of these expenses (Paraszczak, Svedlund, et al., 2014). Additionally, ventilation costs can account for up to 40% of total operating costs (Bharathan et al., 2017). Rising CO2 taxes and increasing renewable energy production capacity are expected to reduce electricity costs, making electric vehicles more cost-effective than diesel alternatives (Sanguesa et al., 2021). To address these challenges, the mining industry is conducting numerous research projects, including a collaboration between Boliden and Sandvik to test a new battery-electric LHD LH518iB (BLHD) in the Garpenberg underground mine in Sweden. The BLHD is powered by lithium-iron-phosphate (LiFeP) batteries that charge and swap at a charging station situated within the mine. Instead of fast charging, Sandvik focused its resources on a swapping system for the batteries. Sandvik's "Autoswap" system allows the operator to swap the battery in less than six minutes (Blinn et al., 2023) (Leonida, n.d.). Despite the challenges, Boliden has set a target to reduce its carbon footprint by 40% by 2030, with 2021 as the reference year. This goal can be accomplished by testing and implementing new technologies that reduce fossil fuel consumption and improve energy efficiency (Boliden Annual and Sustainability Report 2022)

The mine in Garpenberg is one of Sweden's deepest mines, reaching a production depth of almost 1,500 m. Its primary minerals are zinc, lead and silver, whereas its secondary minerals are copper and gold. Its total ore production is about 3.3 Mio tons of ore and is expected to increase in the future (Derrien, 2022).

1.1. Scope of the Thesis

The thesis investigates the simulated battery performance, productivity, energy efficiency and swapping procedures of the battery loader on the parameters of the Garpenberg underground mine. This will be achieved by collecting machine data on the LHDs and investigating different driving patterns. The maximum horizontal and vertical distance between the mine's charging point and face will be simulated and analysed.

In addition, the study will discuss different settings in the simulations, describing the differences between the alternatives and estimating the investment costs and fleet size.

Finally, the study will compare the machine performance metrics of the BLHD with the current non-battery-powered LHDs and estimate the potential impact of converting Garpenberg's entire LHD fleet to battery-powered LHDs in terms of production and the power grid. The results of this study will help mining companies to make informed decisions about the use of battery electric equipment and give references for the design of charging infrastructure in underground mines.

1.2. Out of scope

It should be noted that this study has certain limitations due to the confidentiality requirements of Boliden and Sandvik, which necessitate the exclusion of certain factors and the use of averaged values for others. Further, the impact of the BLHD on the ventilation system will not be investigated, as this is a complex issue that would require more time than is available within the scope of this thesis.

Moreover, the study will not consider the individual operator performance or the experience levels of the operators on both machines. These factors can have a significant impact on the performance of the machines. Additionally, while a cost analysis will be conducted, it will be more detailed for Boliden and RWTH Aachen only. This is because the exact cost information from Sandvik is confidential and cannot be disclosed without an NDA.

1.3. About Boliden

Boliden is a leading mining company in Europe, operating exclusively in the northern region of the continent. The company has four mines and five smelters in Norway, Finland, Sweden and Ireland. It also has four sales offices in Denmark, Sweden, Germany and England (Figure 1). With a total workforce of 6,226 people, Boliden generated revenues of $8.48 billion in 2022. The company produced 353 kt of copper, 475 kt of zinc, 71 kt of lead, 26 kt of nickel, 21,173 kg of gold, and 552,533 kg of silver (Boliden Annual and Sustainability Report 2022). Besides the primary metal production, Boliden is also involved in metal recycling. The company tries to be a front-runner for automation and electrification for both underground and open pit mines (Boliden Annual and Sustainability Report, 2022).

2. Literature Review

At the beginning of the project, getting familiarised with the terms used in electricity, the physical formulas used in battery technology, and their current state of development was the primary focus. Followed by an investigation of previously conducted research on battery-powered vehicles in underground mines. Since battery technology is new in underground mining machines, the information about its performance is still unexplored. Therefore, much information is based on Sandvik's internal investigations and first client experience from New Gold. Multiple meetings and interviews were conducted to exchange knowledge and new developments with stakeholders worldwide.

Furthermore, this chapter discusses the mine design and mining method of the Garpenberg mine and the different machines LH621i and LH518iB from Sandvik. It also gives an overview of the necessary infrastructure around and in the mine that must be included for battery technology.

2.1. Garpenberg Mine

The Garpenberg mine is located in the north-western part of the Garpenberg syncline, about 180 km northwest of Stockholm (Figure 1), and has a rich mining history dating back to 375 BC. It is currently one of the largest base metal mines in the country. The Zn-Pb-Ag sulphide deposits are distributed along the north-western limb of the syncline and have a unique structural orientation reminiscent of upright domes (Tiu et al., 2021). The primary minerals are zinc, lead, and silver, whereas the secondary minerals are copper and gold. In 2022, the total mined-out ore was 3,041 Kton. Of which zinc accounted for about 48%, silver for 32%, lead 13% and copper-gold for 7% of the revenue. These deposits contain significant mineral resources (measured and indicated) with an estimated total value of approximately 21,600 kt at 2.7% Zn, 1.3% Pb, 0.06% Cu, 70 g/t Ag and 0.41 g/t Au (Boliden Annual and Sustainability Report 2022), (Derrien, 2022).

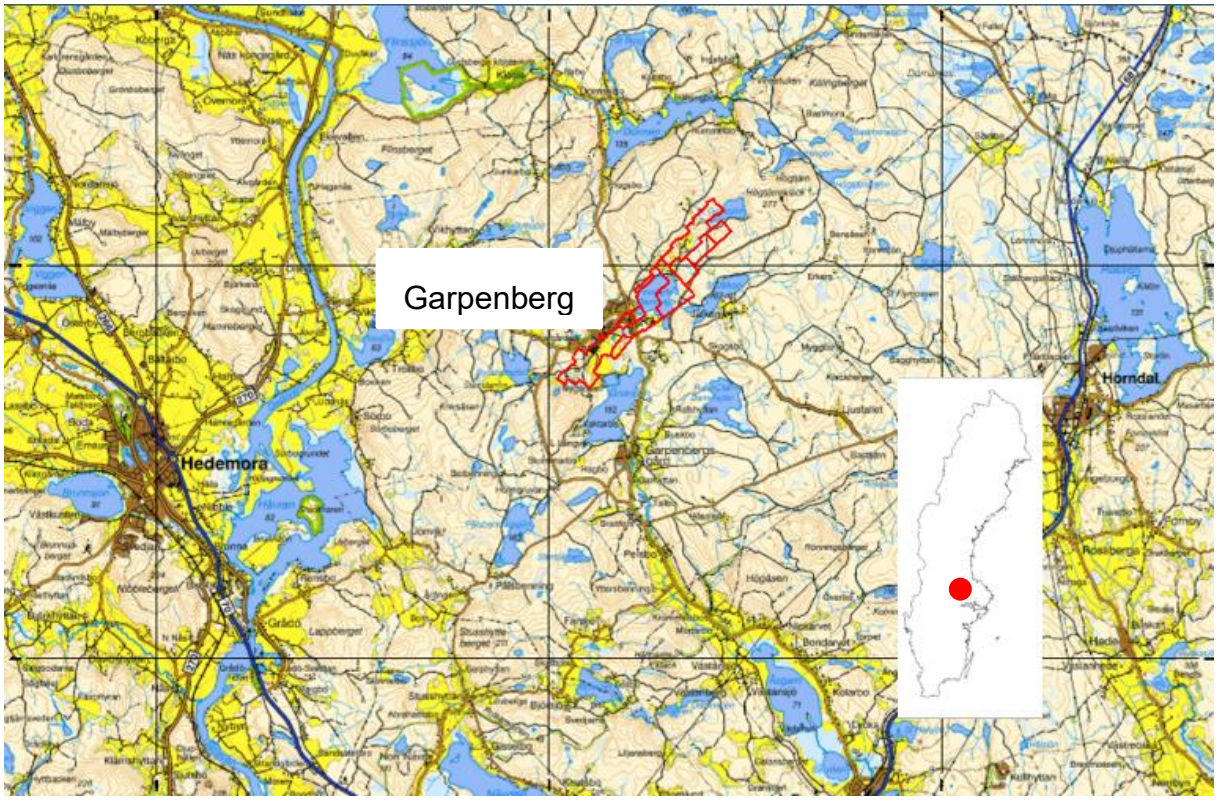

Figure 1: Location of the Garpenberg and the underground mine in Sweden. The coordinate system is RT90 2.5 gon W (Derrien, 2022)

Mining activities at the site primarily focus on extracting ore from Lappberget, while only a quarter of the total amount is extracted from the other deposits. The western and eastern deposits are already depleted, but exploration work is underway at three other sites, with Huvudmalmen being the most significant. The deposit has an east-west extension of about 4,200 m and a north-south extension of about 2,150 m. The deepest point of exploration activity at Lappberget currently reaches a depth of about 1,500 m (Figure 2) (Derrien, 2022).

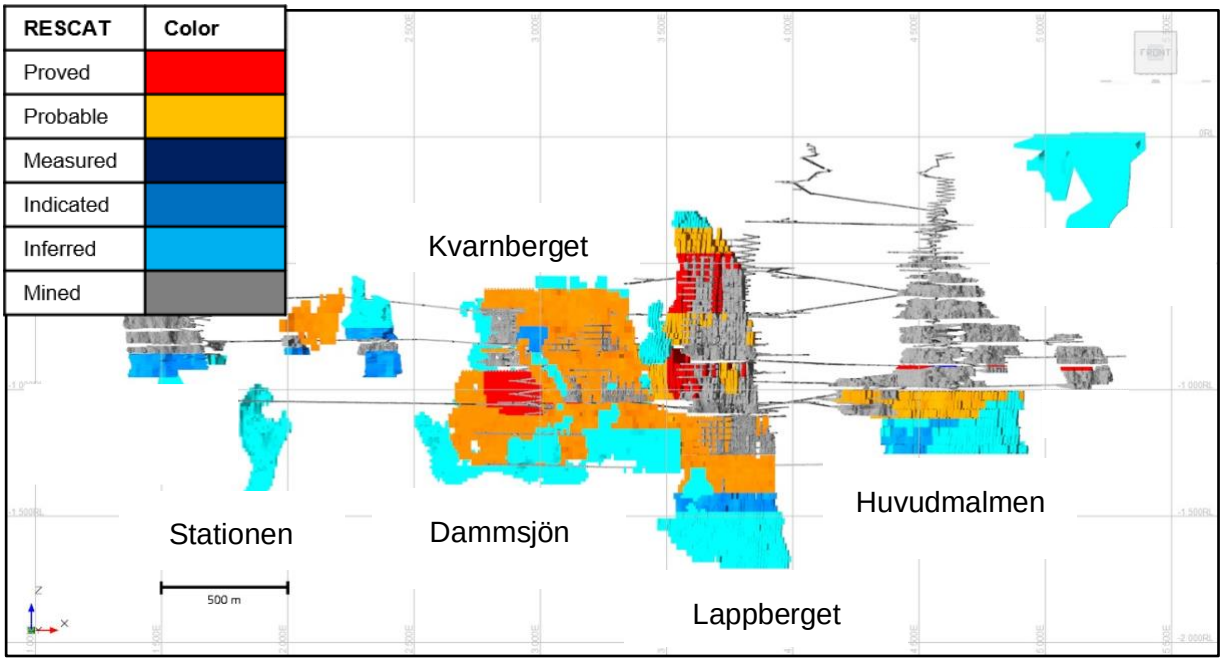

Figure 2: Front view of the deposits in Garpenberg (Derrien, 2022)

2.1.1. Mining method and mine design of Lappberget

Sublevel mining, also known as long-hole mining, is the predominant mining method at Garpenberg, accounting for over 95% of the ore extracted. In this technique, the ore is mined in layers between two vertically spaced adits 25 m to 35 m apart. In most cases, the transverse long-hole heading is used, where the axis of the drift is perpendicular to the strike direction of the ore body. However, in more limited areas, longitudinal long-hole mining is also used, where the mining direction is aligned with or parallel to the strike of the ore body. The primary and secondary stops are mined in a predetermined sequence, forming a pyramidal sequence. The standard dimensions of the stopes are 22-35 m high, 10 m wide for the primary stope and 15 m wide for the secondary stopes, although dimensions may vary locally. The ore bodies are divided into mining blocks, with each block containing 3 to 8 levels of drifts. The uppermost floor of each mining block is the sill pillar, which separates the different mining blocks. The floor above the sill is backfilled with cement paste to allow the mining of the ore remaining in the sill. In addition, a 10-15 m thick sill will remain under old mined-out areas filled with waste rock. This division into different mining blocks allows the mine to plan and operate several production areas simultaneously (Figure 3). Besides sublevel mining, other and rarely used mining methods like cut and fill and Avoca (rill) are being used. However, both methods are only used in the Dammsjön (Derrien, 2022).

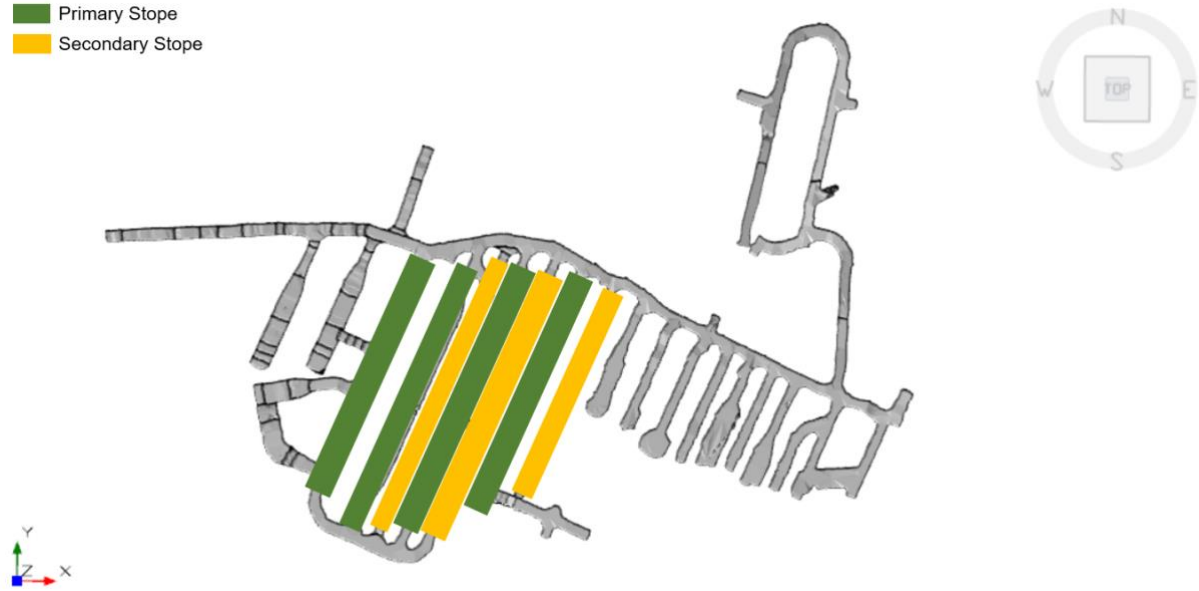

Figure 3: Mining method in Lapperget with primary and secondary stopes

2.1.2. Underground Mining Production Work Cycle

A typical production work cycle in underground mining for mineral ore extraction involves a specific sequence of tasks and machines. It begins with the drilling rig creating blasting holes, which are subsequently loaded with explosives and an igniter. The ore is then blasted, leading to the fragmentation of the working face. Following the blasting, production machines, also known as LHDs, are responsible for mucking the fragmented ore and loading it onto trucks. These trucks transport the ore to the crusher, or the LHDs dump the ore directly in ore passes. Once the drift is emptied, a scaler removes loose rocks from the drift's walls, roof, and face. Shotcrete is sprayed on the walls and roof to ensure rock stability and safety, and bolts are installed for reinforcement. In contrast, when a stop is emptied, it is backfilled using paste (in primary stopes) or waste rock (in secondary stopes) (Figure 3 Figure 4) (Hamrin et al., 2001).

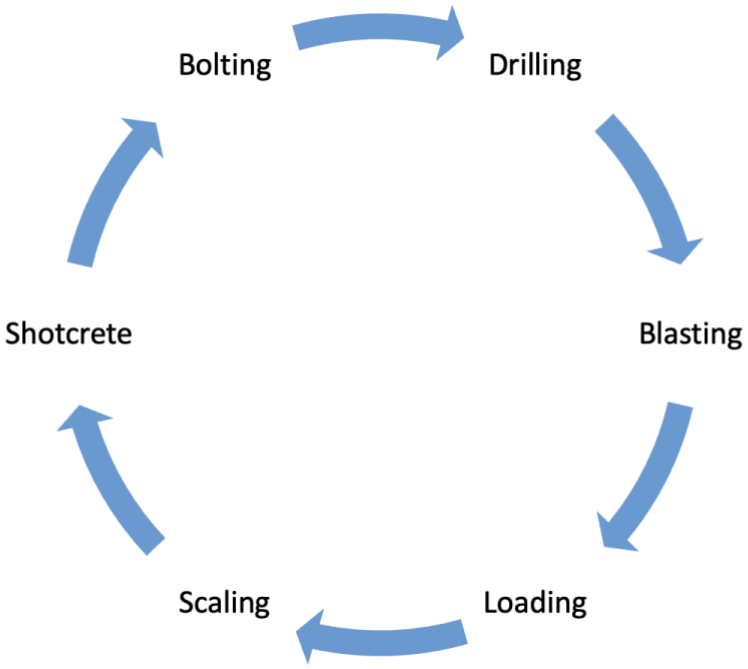

Figure 4: Underground production mining cycle

2.2. Sandvik TORO LH621i

The TORO LH621i underground loader is a high-volume machine designed for fast-moving applications. The hydraulic system offers fast bucket filling and high ramp speeds. Depending on the specification, the loader can be equipped with a Volvo Tier 2/Stage II engine, a Tier 4f engine, or a Stage V low-emission engine for ultra-low sulphur diesel. The loaders used by Boliden are all equipped with the Stage V specification to meet European standards. Currently, Boliden has in total six LH621i loaders operating (Sandvik, 2022c).

Table 1: Dimension parameters for the TORO LH621i underground loader

CATEGORY	VALUE	UNIT
TOTAL WEIGHT	79,800	kg
FRONT AXLE	25,400	kg
BACK AXLE	33,400	kg
DIMENSIONS		
LENGTH	12.54	m
WIDTH	3.195	m
HEIGHT	2.944	m
TURNING RADIUS	7.9	m

In terms of dimensions, the loader has a total operating weight of 58,800 kg. The bucket capacity is 10.4 m^3. The loader's length, width and height dimensions are in Table 1. The maximum lift height of the bucket is 4.817 m, and the machine has a maximum turning radius of 7.9 m. The loader cabin has an air-suspended driver's seat, an adjustable steering column and air conditioning. The cab is also equipped with a ROPS/FOPS certified protective structure that protects in the event of a rollover or falling object. The loader also has a camera system that gives the operator a 360-degree view of the machine (Sandvik, 2022c).

The standard engine is a 6-cylinder in-line Volovo TAD1244VE engine with a maximum power of 2,100 rpm and a torque of 2,005 Nm at 1,260 rpm. The engine has a tank capacity of 760 l and an average fuel consumption of 45 l/h at 50% load. Depending on the engine version, the loader reaches a top speed of 25.9 km/h or 27.8 km/h. The loader's Tier 4f engine is equipped with a diesel particulate filter and a selective catalytic reduction system that reduces particulate emissions, nitrogen oxides and other harmful gases. The Stage V engine is equipped with a diesel oxidation catalyst, a diesel particulate filter and a selective catalytic reduction system, further reducing emissions. However, fuel consumption is one litre higher for the specifications than the standard version (Sandvik, 2022c).

Figure 5: Sandvik's Toro LH621i

Figure 31 lists the grade performance of the LH621i on different inclinations, emptied as well as loaded. The machine has four gears in which it can shift. In Lappberget, the inclination of the ramp on the straight is 1/7; in the curves, it is 1/10 (Sandvik, 2022c).

The loader is equipped with the Sandvik Intelligent Control System, My Sandvik Digital Services, The Knowledge Box onboard hardware and AutoMine readiness. The integrated weighing system is available to measure the payload in the bucket and the number of buckets filled during a shift. SHARK TM ground engaging tools are available for the loader bucket to optimise productivity and extend bucket life (Sandvik, 2022c).

2.3. Sandvik TORO LH518iB

The new battery loader LH518iB is Sandviks' most advanced battery loader for underground operations. This chapter is about the machines' specifications and technology.

2.3.1. General Information

The engineers from Sandvik decided to completely redesign the loader only for electrification purposes and not just use the loader's design based on which the LH621i is based. Sandvik hopes to optimise the loader's performance by redesigning the machine, leading to fewer changes in the mine infrastructure and schedules. With the takeover of Artisan, Sandvik now has a real asset in its portfolio for battery technology and development. Artisan decided to use its batteries based on the Lithium-Iron-Phosphate chemistry and to swap batteries instead of fast charging them. The battery capacity is 353 kWh, supplying the three Permanent Magne

AC motors with electricity. Two motors are installed on the front axle and one on the rear axle. The motors create a total power output of 560 kW, which creates a tractive effort of 460 kN. For the hydraulic part, Sandvik installed two motors with 100 kW each (Bołoz, 2021).

Regarding dimensions, the loader has a total operating weight of 52,000 kg. The bucket size is 8.4 m^3, meaning the loaded weight is 70,000 kg. The loader's length, width and height dimensions are in Table 2. The maximum lift height of the bucket is 4.569 m, and the loader has a maximum turning radius of 7.4 meters. The loader's cabin is designed similarly to the LH612i loader (Sandvik, 2020) (Figure 6).

Table 2: Dimension parameters for the TORO LH518iB underground loader

CATEGORY	VALUE	UNIT
TOTAL WEIGHT	70,000	kg
FRONT AXLE	19,000	kg
BACK AXLE	33,000	kg
DIMENSIONS		
LENGTH	12.54	m
WIDTH	3.195	m
HEIGHT	2.944	m
TURNING RADIUS	7.4	m

The TORO LH518iB is an upgraded version of the LH518B. The upgrade does not impact the performance or power of the machine but the maintainability and reduces attrition of the frame. Furthermore, it now has the capability to use Automine.

The grade performance of the LH518iB is 11.5 km/h loaded and 14 km/h unloaded at a maximum inclination of 20 degrees. The loader can reach a maximum speed of 27.5 km/h loaded and 28.3 km/h unloaded on an even terrain (Figure 32).

Figure 6: Side view of the battery loader LH518iB

2.3.2. Battery Technology

The LiFePO4 battery case was created and constructed by Artisan and is composed of three packs - two main packs and one tramming pack. Its total energy capacity is 353 kWh, with a peak output of 660 kW and a continuous output of 560 kW. The battery can be charged with a current of 2x 300 A, and the ideal charging power is 2x 180 kW, which takes about 60 minutes to charge the battery from zero to 100%. The battery weighs 9 950 kg and uses a liquid cooling system to regulate its temperature, ranging from 55 C to -22 C. Besides the main battery, the loader has one auxiliary battery with a capacity of 576 Ah to manoeuvre the machine in the swapping process (Sandvik, 2020, 2022)).

The Artisans battery system design comprises four stages that ensure the safe and efficient functioning of the battery. The first stage is the battery cell, which stores chemical energy and facilitates the reaction between the cathode and anode. Isolation layers protect the cell, and a laser-welded aluminium case prevents any leakage of the battery contents. Additionally, each cell is equipped with pressure vents to prevent any possible bursts that may occur (Sandvik, 2022).

In the second stage, multiple cells are combined to form a module. This module operates at relatively low voltages, usually around 40 V, to ensure a safer and more reliable service. The

module also includes temperature monitoring sensors and cooling to ensure the cells do not overheat or become damaged during operation. The temperature sensors monitor the temperature of the cells and trigger the cooling system when necessary to prevent any damage (Sandvik, 2022).

In the third stage, multiple modules are combined to create a battery pack. This casing is designed specifically for mining purposes and is fabricated with 6 mm steel plates to provide maximum protection. The casing is strategically sealed with drains that allow fluids to drain without the ingress of dust and contaminants. The cooling system within the casing is a non-conductive coolant that manages the temperature during charging. Additionally, the battery pack contains a Battery System Controller (BSC) that monitors all safety thresholds and disconnects battery contractors if required. An Isolation Monitoring Device (IMD) also monitors the electrical isolation between the high-voltage circuit and the chassis. Furthermore, the battery pack includes 600 A fuses that protect against overcurrent and damage from external shorts (Sandvik, 2022).

In the final stage, the battery pack is stored in a safety cage that is a robust mechanical steel cage. This cage protects the battery pack from rockfall and crushing, making it ideal for use in mining environments. Additionally, the cage design favours the autonomous autoswap of the battery without putting the operator in danger, making it safer and more efficient (Sandvik, 2022).

2.3.3. Safety Measures

The battery loader engineers prioritised safety by developing a battery design with a safety strategy for thermal runaway prevention, which aims to prevent gas and fire occurrences (Sandvik, 2022b). This approach involved minimising the likelihood of a thermal runaway event through the design, utilising intrinsically safer chemistry to reduce the severity of such an incident, and implementing containment and suppression measures to mitigate any adverse consequences.

The likelihood of battery damage can be reduced by engineering the battery's cells, modules, packs, and cage to withstand heat, deformation, and vibration. In addition, implementing internal ventilation systems and sensors, such as Battery Management Systems (BMS), BSC, and IMD, safeguards the battery against overheating, charging or short-circuits, and other related concerns (Sandvik, 2022).

In the event of smoke, fire, or a battery burst, the severity of the incident can be reduced through the utilisation of safer chemical compositions such as LiFePO4. Lithium-iron-phosphate produces significantly lower heat levels than other alternatives, like nickel manganese and cobalt (NMC) or lithium cobalt oxide (LCO). Furthermore, this chemical composition generates minimal gases, with most of the gas resulting from materials such as electrolytes, plastics, rubber, and paint. However, it is essential to note that the formation of hydrogen fluoride (HF) is a possible chemical reaction that must be taken into consideration. This can occur when fluorine ions in the electrolyte combine with hydrogen atoms from water (Sandvik, 2022).

To counteract any potential adverse outcomes, an internal fire suppression system has been developed that is thermally activated and can effectively suppress fires in the initial stages without causing damage to the pack's internal components. This innovative technology uses an aerosol agent that chemically interrupts combustion and fills the inside of the pack without damaging it (Sandvik, 2022).

2.4. Infrastructure

An underground mine such as Garpenberg requires much infrastructure. In the following, the mine layout, road conditions and an electricity plan are laid out.

2.4.1. Mine Layout

Lappberget mine is stratified into etages, each comprising multiple levels, with each level housing various drifts and stopes. Currently, the mine is organised into seven etages, with the highest level situated at a depth of -325 m and the lowest at -1,450 m. The levels are interconnected through a ramp that extends to the surface, facilitating the movement of ore, materials, and personnel in and out of the mine. In addition to the ramp, there are two shafts for transporting ore and personnel. The ore hoist reaches from the surface to -1,175 m, while the personal hoist terminates at -1,054 m but also stops at depths of -560 m, -700 m, and -864 m. The underground head office is located at level -1,054 m. Bolts, meshes, and shotcrete for rock support reinforce the roof and walls of the mine (Derrien, 2022).

2.4.2. Road Condition

The main roads in the mine are kept in good condition by the maintenance group, ensuring safety and allowing a maximum speed of 30 km/h. However, the road conditions deteriorate in the mucking area, making it difficult to maintain this speed. The mine design is not optimal for loader operations due to narrow curves and washed-out roads, causing significant strain on the machines, which can weigh loaded over 70 tons. Over time, the roads become uneven and require frequent repairs by loader operators or the road maintenance crew, further reducing their production time and negatively affecting the WCT (Figure 7). The time needed to repair the reads can take a couple of hours or sometimes a whole shift, depending on the damage's size (Mining Engineer, personal communication, April 2023).

Figure 7: Road condition in the Garpenberg mine: on the ramp, before the ore pass and in the drift

2.4.3. Energy Grid

The mine consumed 2,788 m^3 of diesel fuel for mobile equipment last year. The load and haul process accounted for 81% of the fuel usage, the mucking process with loaders accounted for 28%, and the hauling process with trucks accounted for 53%. The remaining energy consumption was attributed to auxiliary machinery, mining, and construction processes. In the long term, Boliden plans to replace all diesel-powered mining equipment with electric engines. However, this transition would require a significant amount of electricity, with an estimated demand of 10.9 GW solely for supplying electricity to mobile mining equipment and pickups. Specifically, 3.08 GWh and 5.74 GWh would be needed for the loaders and trucks, respectively. This calculation is based on the current diesel consumption and an improvement factor of 0.4 in battery efficiency over time (ABB, personal communication, April 2023).

Figure 8: In the Garpenberg mine the power distribution bay on level -1232 m

The underground power grid has a total capacity of 10 KV, consisting of three major power lines coloured orange, blue, and pink. Each of these power lines has a capacity of 12 kW. At level -1,232 m, there are three converters. Two of these converters have an output of 400 V, which supplies electricity to the charging bay and ventilation, while the other converter has an output of 1000 V, which is necessary to power mobile mining equipment such as the drill rigs (Figure 8) (Electrician Engineer, personal communication, May 2023).

2.4.4. Charging and Service Bay

The LH518iB employs a battery-swapping technique to tackle the issue of insufficient battery capacity to sustain an entire eight-hour work shift. Therefore, the location of the charging bay needs to be considered with the utmost caution.

Several essential factors must be considered for the design of the charging bay. The size of the bay can vary, but it must not be less than 8.5 m in width, 18 m in length, and 3 m in height. The dimensions of the charging bay at Lappberget are 10 m wide, 20 m long, and 6 m in height. Additionally, it has a power supply of over 1000 V, internet access, and proper ventilation to maintain a temperature of 25°C. The entire bay is supported by roof bolts, meshes, and shotcrete, similar to the rest of the mine. Furthermore, the floor is constructed of concrete and is levelled out, with appropriate safety measures in place in case of a fire, including installation on the walls and roof (Sandvik, 2022a)(Figure 9).

Figure 9 shows the two charger units and one cooler unit, which are required to recharge the battery. The charging units have 3 x 1.5 m dimensions in all three directions and weigh 2,500 kg. Their optimal operating temperature should be between 10°C and 40°C. The altitude should not exceed -2,000 m to 2,000 m, as power loss would be inevitable outside of this range. The ideal humidity range for the charging units is between 30% and 100%. The chargers have a constant maximum output of 320 kW. During the charging process, the battery's temperature increases. A cooling unit, which has almost the same dimensions as the charging unit but weighs 1,100 kg, is required to reduce the temperature. Like the charging unit, it has the same environmental requirements (Akimsar, n.d.).

Figure 9: Charging Bay design on level -1232 m

The loaders operate in the harshest environment without any rock support and bad road conditions. Hence, it is very likely that they will get damaged by rockfalls and have high attrition. To ensure a quick repair and service of the machines in the mine, Boliden has a services bay on the same level as the charging bay. One corner has been cleared for the new BLHD only to ensure quick and smooth repair and maintenance for the loader (Figure 10).

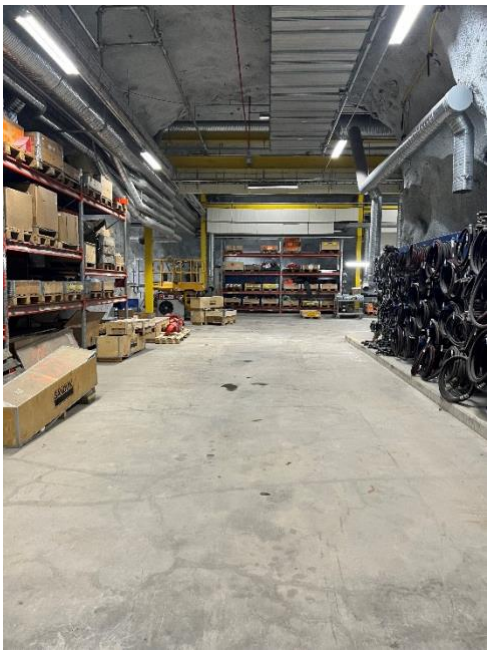

Figure 10: Maintenance Bay on level -1232 m

3. Methodology

Integrating novel technologies into an operational underground mine poses multiple challenges. Consequently, management must consider the salient factors of general expenses and machine productivity as primary concerns (Nieto et al., 2020). Simultaneously, understanding the prerequisites and limitations necessary for successfully implementing the new technology is essential. The ensuing discussion presents a methodology for delineating Key Performance Indicators (KPIs), the software of choice, selected configurations, established infrastructure, and anticipated expenditure (The Electric Mine, 2022).

3.1. Machine Performance Metrics

To perform a comprehensive comparative analysis of both technologies and their impact on the Garpenberg underground mine, a set of Key Performance Indicators (KPIs) has been identified. These KPIs encompass essential metrics, including available hours, downtime, utilized hours, idle time, productivity, and energy efficiency. The LH621i technology's real performance data will be utilized for reference.

Additionally, interviews with New Afton and Sandvik representatives will be conducted to gather valuable insights and information regarding the LH518B technology. Notably, the LH518iB loader faced delays in arriving at Garpenberg due to supply chain issues, resulting in a lack of direct performance data.

In light of this limitation, the performance data for the LH518iB loader will be calculated using the specialized software Vehicle Performance Calculator (VPC) developed by Sandvik. In cases where specific values cannot be obtained through VPC, they will be estimated using data from New Afton.

3.1.1. Availability and Utilization

Availability concerning the operation of vehicles in the mine is a measure that takes into account the amount of time the vehicle is allowed to work, regardless of its ability to work, and compares this with the amount of time it is both allowed and able to work, i.e. available. This ratio is calculated by dividing the total time the unit was allowed and able to work by the time the vehicle was available to work (Nieto et al., 2020) (The Electric Mine, 2022) (The Operational Definitions and KPIs Sub-Committee, 2020).

To define availability, three parameters are considered:

1. Rostered Hours: This refers to the total time the mine was in operation and the vehicle was potentially available for work (Nieto et al., 2020).
2. Lost Time: Lost time is the time when the vehicle cannot work due to unforeseen obstacles or events. It includes different types of delays, such as unscheduled time, scheduled maintenance time, unscheduled maintenance time, set-up and adjustment time, idle time without an operator, waiting time, loss of loading time, loss of time due to working conditions and loss of speed (Nieto et al., 2020).

3. Downtime: Downtime is the time during which the vehicle cannot be operated due to equipment failure. However, it is essential to note that certain activities, such as refilling the fuel tank or charging the battery, are considered downtime but can be performed during the vehicle's scheduled idle time. For example, if a shift lasts eight hours and the unit is only in use for four hours, the remaining four hours are considered idle time, during which the vehicle can be prepared for the next operation. In this way, the idle time during scheduled shifts appropriately impacts the vehicle's availability and utilisation (Nieto et al., 2020).

Equation 1: Availability of mining equipment (A)

$$A\ (\%) = \frac{rostered\ hours - downtime - lost\ time}{rostered\ hours - lost\ time} x100 \quad (1)$$

Availability utilisation is a key figure that takes into account the already mentioned idle time of a vehicle. It not only considers whether a vehicle is allowed and able to work but also evaluates the percentage of available time that the vehicle was actually in operation. In other words, it measures how efficiently the vehicle used the time it was available to work.

To calculate the utilisation of availability (UoA), the time the vehicle was in operation is divided by the total time it was allowed and able to work. This ratio provides information on how effectively the vehicle's operating hours were used (Nieto et al., 2020)(The Operational Definitions and KPIs Sub-Committee, 2020):

Equation 2: Utilization of the availability of mobile mining equipment (UoA)

$$UoA\ (\%) = \frac{restered\ hours - downtime - lost\ time - idle\ time\ (h)}{rostered\ hours - downtime - lost\ time\ (h)} x100 \quad (2)$$

The concept of Mean Time Between Failures (MTBF) focuses on evaluating the reliability of equipment. It involves calculating the average time that elapses between successive failures of a particular piece of equipment over a specified operating period. MTBF takes into account the number of failures the device experiences within a given number of hours of operation. By determining the average time between these failures, MTBF provides an estimate of the expected operating time of the machine before another failure occurs. This metric is valuable for predicting equipment reliability and helps with maintenance planning to minimise downtime and improve overall efficiency (Nieto et al., 2020)(The Operational Definitions and KPIs Sub-Committee, 2020). Mathematically, the MTBF can be expressed as:

Equation 3: Mean Time Between Failure of Mobile Mining Equipment (MTBF)

$$MTBF = \frac{restered\ hours - downtime - lost\ time - idle\ time\ (h)}{failure\ frequency} \quad (3)$$

Mean Time To Repair (MTTR) is vital in understanding how quickly the equipment can return to regular operation after an incident. It plays a critical role in maintenance strategies, as minimising MTTR can reduce downtime and improve overall operational efficiency (Nieto et al., 2020).

Equation 4: Mean Time To Repair of Mobile Mining Equipment (MTTR)

$$MTTR = \frac{repair\ hours}{failure\ frequency} \quad (4)$$

However, both values need to be considered cautiously because the MTBF is an average, which does not consider the length to repair, and the MTTR does not consider that incidents happen irregularly (Nieto et al., 2020).

3.1.2. Productivity

The comparison of productivity between the two loaders presents a considerable challenge due to the necessity of considering multiple influential factors and the requirement for maintaining a closely analogous environment to ensure the comparability of data resulting from calculations.

To quantify the productivity of the machines in various scenarios and simulations, the subsequent formulas are employed:

- The WCT is a highly sensitive metric influenced by variables such as machine power, road conditions, layout, speed, and operator proficiency. Employing statistical assessment of numerous work cycles mitigates the impact of fluctuations and allows the identification of trends(The Electric Mine, 2022). Mathematically, the WCT is formulated in the following :

Equation 5: Work Cycle time of Mobile Mining Equipment (WCT)

$$WCT = Mucking + Tramming + Dumping + Tramming \quad (5)$$

- The calculation of average speed for distinct work cycle scenarios involves the application of the subsequent formula to each segment of the work cycle:

Equation 6: Work Cycle Speed of Mobile Mining Equipment (WC Speed)

$$WC\ Speed = \frac{Distance}{Speed} \quad (6)$$

- The Bucket Fill Factor (BFF) hinges on attributes such as bucket size and characteristics of the ore material, including fragmentation, density, and moisture content. To calculate it, knowledge of the swelling factor is essential. This factor is determined through the formula (Mousa Mohammadi, Suprakash Gupta, Piyush Rai, 2015):

Equation 7: Bucket Fill Factor (BFF)

$$BFF = \frac{Volume\ of\ material\ in\ the\ bucket}{bucket\ capacity} \quad (7)$$

In this situation where the swelling factor for the Garpenberg ore is unknown, the average capacity is calculated as a percentage and then applied to the bucket size of the battery loader to approximate the bucket fill factor.

- The Performance rate offers insights into the operational efficiency during shifts. It delineates the ratio between the actual output and the maximum potential production. Caution is warranted in interpreting this value as it can vary based on machine attributes, environmental conditions, and operator skills. The following equation describes the PI (Mousa Mohammadi, Suprakash Gupta, Piyush Rai, 2015):

Equation 8: Performance Rate (P)

$$P = \frac{Actual\ Production\ (Output)}{Potential\ Production\ (Rated\ Output)} \quad (8)$$

- To facilitate a comprehensive overview and comparison of the aforementioned KPIs, the Overall Equipment Effectiveness (OEE) coefficient serves as an encompassing metric. Widely adopted in production industries, the OEE assesses effectiveness, utilization, and availability. Various methodologies exist, but the formula introduced by Samanta and Banerjee (Samanta & Banerjee, n.d.) was selected for this study because they have given weights to the factors to make it more realistic for the mining industry since the original equation from Nakajima (Nakajima, 1988) is used mostly in the manufacturing and processing industry and have equal rates.

Equation 9: Overall Equipment Effectiveness (OEE)

$$OEE = A^{0.3} * U^{0.5} * P^{0.2} \quad (9)$$

3.1.3. Energy Efficiency

To assess the energy efficiency and loads handled per shift for the LH621i and LH518iB loaders, both were evaluated using dedicated software Optimine for the LH621i and VPC for the LH518iB. The Net Energy per ton is determined by dividing the total net energy consumption per shift by the total material moved during the shift:

Equation 10: Net Energy efficiency function for loaders (NE)

$$NE = \frac{Net\ Energy\ (kWh)}{Total\ shift\ tonnage(t)} \quad (10)$$

3.2. New Afton Mine

The New Afton Gold Mine, owned by New Gold, is a mine located in British Columbia, Canada. The mine is situated approximately 10 kilometres west of Kamloops and is recognised for its significant gold, copper, and silver reserves (Lecuyer et al., 2020). The mine is about 700 m deep and uses the block-caving mining method to extract the ore (Cancino Martínez et al., 2022).

In 2021, the mine implemented the utilisation of the TORO LH518B battery loader, procured from Sandvik, to enhance its electrical mining operations. Extensive trials were conducted to evaluate the loader's performance, utilisation efficiency, and environmental impact. The company conducted comparative assessments between the LH518B and their standard CATR29000 loader by traversing a predetermined route with a fixed amount of material over a distance of 432 m, featuring a gradient of 13%. The evaluation encompassed evaluating regeneration capabilities during both the ascent and descent of the ramp(Acuña et al., 2022).

The conducted tests have yielded significant insights into the performance improvements brought about by the battery loader technology. Specifically, the WCT witnessed a notable 2% enhancement. The speed of the battery loader displayed a remarkable surge of 60%. Furthermore, the battery loader showcased an approximate 20% increase in the number of handled buckets, indicating heightened efficiency in material handling tasks. However, the bucket size differs between 6,6 and 9,2 m between the battery loader and the caterpillars (C. Gamble, personal communication, April 2023) (Acuña et al., 2022).

An impressive attribute of the battery loader is its capacity to regenerate a portion of expended energy to replenish its battery. This regeneration process exhibited an efficiency rate of 37%, underscoring the technology's ability to harness and repurpose energy during its operational cycle.

It is worth noting that the battery loader's average power output is nearly twice that of the Caterpillar machine, showcasing its robust energy demand. However, despite this higher power output, the battery loader consumed approximately four times less energy during testing compared to the Caterpillar machine (Acuña et al., 2022).

Furthermore, the environmental contrast between the two technologies is stark. While the battery loader demonstrates negligible or non-existent heat and gas emissions, the Caterpillar machine (CATR29000) emits 3.3°C and 292% more heat and DPMs (Acuña et al., 2022).

To swap the 10-ton battery pack, Artisan developed the Autosawp system, which allows the battery to be changed while the operator sits in the safe cabin. The machine has two hooks and a pin system to raise, lower and lock the battery pack to and from the machine. The margin for error is relatively small, so good visibility, level ground and adequate room to manoeuvre are important. Initially, operators at New Afton had some problems with the autoswap mechanism because the battery was not level enough. This resulted in several attempts and longer swapping times. One problem was that the hooks did not fit into the correct holes in the battery housing.

Figure 11: Images of the Autoswap process and its complications when vehicle and battery are not aligned (sent from New Afton)

This issue prompted the development of a "kickstand" mechanism to rectify battery positioning and ensure smoother swapping, even on imperfectly level surfaces (Figure 11 Figure 12) (C. Gamble, personal communication, April 2023). In Figure 12 the red flags help the operator to navigate better.

Figure 12: Installation to improve battery swap (sent from New Afton)

The installation of a JIB arm in the charging bay of the Z50 haul truck at New Afton facilitated operator ergonomics and facilitated the management of heavy cables. This JIB arm will also

be implemented in the new charging bay intended for the LH518B loader (Figure 13) (C. Gamble, personal communication, April 2023)

Figure 13: Charging Bay layout of the Z50 haul truck with installed JIB arm (sent from New Afton)

3.3. OptiMine

OptiMine is an advanced software application developed to analyse and improve the efficiency of underground hard rock mining. The software is able to capture machine data in real-time and present it in visual representations or export it as CSV files. At Boliden, OptiMine enables the creation of production, utilisation and signal reports of loaders and drill rigs (ROCKTECHNOLOGY.SANDVIK, n.d.).

The production report consists of three parts: a visual report, a machine comparison and a summary. The report contains both target and actual data for weighing results in tonnes, the number of buckets used, and the average bucket capacity, also measured in tonnes.

The utilisation report includes a breakdown of the total time since the beginning of the service of the machine in the categories of operational, idle and downtime.

The signal report summarises data from various sensors installed in the machines, including temperature values of the machine, oils and hydraulic fluids, average speed, fuel consumption, distance travelled and other relevant measurements.

The software collected the machine and performance data from the TORO LH621i loader. Exported as Excel sheets, the data is then displayed and analysed in Excel and with Python to investigate the KPIs.

3.4. VPC Software

The Vehicle Production Calculator (VPC) developed by Artisan is a specialised program designed to assess the performance of Artisan's battery-powered mining vehicles, including the new battery loader LH518iB. The software takes into account various input data categorised into three groups: mine variables, vehicle variables, and route parameters. These parameters can be adjusted to meet the specific requirements of Sandvik, the client and provide estimations tailored to their needs (Sandvik USA, personal communication, May 2023).

The software generates output results in both PDF and CSV formats. The first page of the PDF report includes a table presenting information about the driving route. The route is divided into segments, each displaying details such as distance, average speed, and inclination. Additionally, this table is accompanied by two 2D graphs:

The next graph visualises the relationship between the route's elevation and distance, allowing for a better understanding of the terrain characteristics encountered by the vehicle.

The last graph illustrates how the vehicle's speed varies throughout the route, providing insights into its performance under different conditions.

On the second page of the PDF report, a graph showcases the State of Charge (SOC) status, WCT, and battery swapping time. This graph helps evaluate the battery's performance throughout the route.

Finally, the report concludes with two tables that summarise the VPC calculations. These tables provide an overview of the machine's and battery's performance, allowing stakeholders to assess the efficiency and productivity of the battery loader LH518iB based on specific parameters and requirements.

3.5. Parameters

In the current version of the VPC software, certain physical calculations such as curves, acceleration and braking time, and speed differentials are not taken into account. Additionally, the software assumes a single value for both mucking and dumping time without distinguishing between the two processes. These limitations may result in some simplifications and potential deviations from real-world scenarios.

Based on the observations from the control room in Lappberget, certain average speeds have been determined for different scenarios. In the drift, the maximum speed is capped at 8.5 km/h, while the curve speed is set to 3 km/h, and in the stope, it is 5 km/h.

Additionally, a brief time study has shown that mucking takes approximately 1 min and 30 sec while dumping takes around 30 sec. These values are used as estimates for the time required for these processes in the VPC software.

Furthermore, the observations have identified various time losses that occur regularly during operations. These time losses include factors such as lost connection, error warnings, scanning the stope, refuelling, cleaning the sensors, and road maintenance. The calculations include an idle time of 1 min per work cycle to account for these time losses. This idle time reflects the typical time losses experienced by the battery loader LH518iB and other vehicles.

3.5.1. Mine variables

Table 3 lists the overall mine parameters that are applicable to each simulation. Among these parameters, the dumping method is the only one that may vary for different scenarios. The available choices for the dumping method are ore pass, remuck bay, or truck, which are determined based on the program and the specific mining method employed. In the case of Garpenberg, LHDs only dump their load in ore passes or remuck bays, as per the mine plan and design. Note that a shift in Garpenberg lasts 9.5 h, while the shift time for the LHD is 8 hours because some time loss occurs due to lunch break and travel time. These values are based on observations and interviews that were conducted while working on-site.

Table 3: Mine site-specific variables

CATEGORY	PARAMETER	VALUE	UNIT	DESCRIPTION
OPERATIONS	*Mine speed limit*	30	km/h	Maximum speed allowed
	Route cycle idle time	1	min	Estimated average time per route cycle for remote driving
LOADING	*Load and dump time*	2	min	Estimated value for loading and dumping per haul
	Default load weight	18	t	Default load weight
DUMPING	*Default dump method*	Ore pass		Dumping method used
GOALS	*Shift goal tonnes*	4000	t	The goal for the production per shift
	Availability	82	%	Percentage of the vehicle up-time per shift
SCHEDULE	*Shift hours*	8	h	Production time per shift
	Shift per day	2		Number of production shifts per day
	Working days per year	360		Number of production days in a year
MINE CLIMATE	*Temperature*	25	C	Temperature in the mine

3.5.2. Vehicle Parameters

When setting up the vehicle parameters in the VPC software, most of the values are predetermined by the manufacturer. However, a few parameters can be adjusted, including the battery capacity, speed limited, rolling resistance and swap time.

In the case of Sandvik's battery loader LH518iB, the battery capacity can be customised. Although Sandvik's battery supplier has developed a new battery pack with a larger capacity of 483 kWh, it is not yet available on the market. Therefore, the calculations in the VPC software are based on the smaller battery pack, which is 353 kW.

The maximum speed of the machine is 29 km/h, but this will be adjusted for each individual segment. Also, VPC will change the speed on inclines according to Table 4.

The rolling resistance, a crucial factor affecting energy consumption, is a key consideration in road design and maintenance. In the case of Garpenberg, it is assumed that the rolling resistance for compacted gravel roads is 3% (Kunze et al., 2002). This value is also utilised by Sandvik (Table 4) when no specific information about the mine road condition is available. The adoption of a 3% rolling resistance assumption is supported by the Global Mining Guidelines Group (The Electric Mine, 2022), which underscores its applicability and relevance in similar mining contexts.

Furthermore, the swapping time for the battery is an important parameter to consider. Based on timing measurements by new Afton and Sandvik, it was determined that a skilled operator could complete the battery swap in 6 min, while a beginner may take up to 20 min. As an average value for the first year, it was assumed that the battery swapping time would be approximately 10 min (Table 4) (C. Gamble, personal communication, April 2023)(Acuña et al., 2022) (Sandvik, 2020).

Table 4: Specific vehicle parameters

CATEGORY	PARAMETER	VALUE	UNIT	DESCRIPTION
VEHICLE PARAMETERS	*Speed*	29	km/h	Maximal machine speed
	Rolling resistance	0.03		Coefficient of friction of the tries
	Battery Energy	353	kWh	Charge Capacity
	Upper Limit	95	%	Battery usable capacity upper limit
	Lower Limit	10	%	Battery usable capacity lower limit
	Discharge Limit	550	kW	Battery discharge power limit
	Power Aux	265	kW	Battery charging power limit
	Vehicle weight	48	t	The weight of the vehicle
	Swap time	10	min	Time required to swap the battery

Load limit	18	t	Maximum load of the vehicle

3.5.3. Work Cycle Parameters

Table 5 presents the WC for the simulation and outlines the parameters that influence the WC. The table consists of eight columns, each containing specific information:

The first column represents the initial SOC and battery temperature at the beginning of each WC. These values can be adjusted based on factors such as the charging philosophy, mine climate, and travel destination. To prevent cell damage from overloading, Sandvik limits the maximum SOC to 95 %. In situations where the SOC reaches this threshold, the machine enters a protective mode, the speed to 1 km/h. The mine climate and the charging rate determine the starting battery temperature. Considering Boliden's decision against fast charging and the relatively stable mine climate at 25°C, a conservative assumption of 25°C is adopted for achieving optimal battery temperature.

The second column denotes the categories that contribute to the calculation of the WC. These segments are further divided into loading, dumping, and tramming activities. Each segment is defined by various parameters, including distance, grade (slope), elevation, and average speed. These values may vary depending on the driving route and prevailing conditions. It is important to note that segments 1 and 6 serve as placeholders for separate charging/parking routes, and thus, they do not contain any specific values here.

Table 5: Example of the WC parameters

WORK CYCLE	**CATEGORY**						
STARTING SOC	*Segments #*	1	2	3	4	5	6
95%	*Distance [m]*	0	100	50	50	100	0
STARTING BATTERY TEMPERATURE	*Grade [%]*	0	0	0	0	0	0
25 C	*Elevation [m]*	0	0	0	0	0	0
	Average speed [km/h]	0	5	7	7	5	0
WAYPOINTS		Charging	Mucking	tramming	Dumping	tramming	charging

The battery loader LH518iB is parked and charged in the charging bay after each shift, ensuring a full battery at the start of every shift. A subroute is designed and considered in the simulation to account for the time and state of SOC loss during the tramming process to and from the charging bay.

The table related to this process consists of five columns (Table 6). The first column of the table is dedicated to defining the charging limit and cooling temperature. These values determine the maximum SOC allowed during the charging process and the desired temperature for cooling the battery (Table 6).

The second column of the table resembles the previous table and includes segments that represent different parts of the route. Segments 1 and 3 correspond to the ramp sections, while segment 2 represents the distance between the ramp and the charging bay located at level – 1,232 m. It is worth noting that the values in segment 2 remain constant and do not change. However, segments 1 and 3 values will vary depending on the specific mucking location (Table 6).

Considering the information within these segments, the VPC software can calculate the time and SOC loss associated with the tramming process to the charging bay and back. These calculations contribute to a more accurate estimation of the overall performance and efficiency of the battery loader LH518iB during its operational cycle.

Table 6: Example of the charging route

CHARGING/PARKING CYCLE	**CATEGORY**			
CHARGING LIMIT	Segments #	1	2	3
95%	Distance [m]	2500	100	2500
COOLING TEMPERATURE	Grade [%]	-14,3	0	14,3
25 C	Elevation [m]	-354	0	354
	Average speed [km/h]	29	5	16,9

3.6. TORO LH621i Scenarios

In the following, various scenarios of LH621i operation are explained, each occurring at different levels of the underground mine. These scenarios serve different objectives and involve distinct driving patterns.

Table 7 enumerates the primary objectives governing the selection of the level and stope. Additionally, a critical consideration was ensuring that the machines designated for operation within the stope possessed functional access to Optimine for the purpose of data collection.

Table 7: Objectives for the TORO LH621i scenarios

SCENARIOS	S-WC	RE-WC	L-WC	AB-WC
WC DISTANCE [M]	200 - 400	200 – 400	500 - 800	500 - 800
TOTAL TONNAGES [T]	8,000	8,000	8,000	8,000
DUMPING METHOD	Ore Pass	Remuck Bay	Ore Pass	Ore Pass
TIME FRAME	April to June	April to June	April to June	April to June

3.6.1. Short WC Distance

On level -801, stope 23 successfully meets all the specified criteria. This WC distance spans approximately 300 m. The distance covered during excavation within the stope is around 100 m and slowly increases. In contrast, the distance covered within the drift, which includes reversing out of the stope and the ore pass drift, is approximately 50 m (Figure 14). From April 21st to May 1st, 2023, three distinct LH621i loaders (designated as FL2, FL3, and FL4) were allocated to carry out tasks.

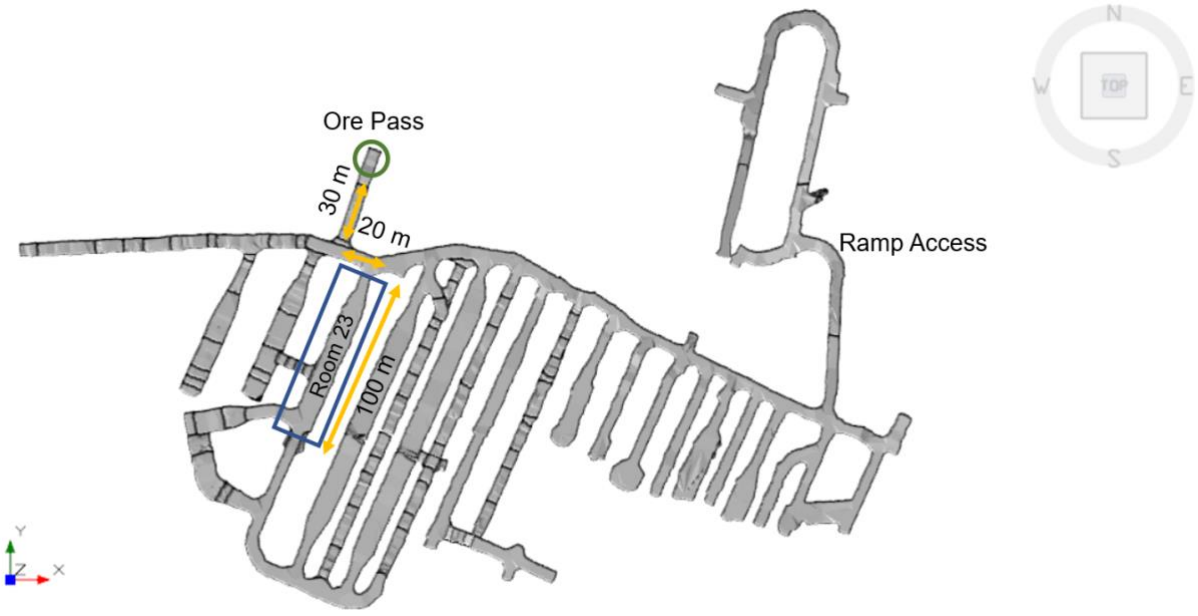

Figure 14: Driving route on level -801 m, short distance WC

3.6.2. Remuck Bay

In Lapperget, not every level has an ore pass or sometimes ore passes are not available. Hence, the ore has to be stored in a temporary bay, also called a remuck bay (Figure 30). These bays are often reinforced drifts in which it is safe to operate with normal loaders and trucks. After the storage room has been filled, the contractor Långdahls Åkeri AB takes over, remucks the ore and loads it onto trucks transporting it to the crusher.

On level -752, stope 18 meets all the specified criteria successfully. The ore pass was unavailable due to it being full. The average work cycle distance remains at 240 m. However, the distance decreases over time due to limited space in the drift compared to the volume of ore in the stope. Consequently, the average driving distance within the stope is approximately 40 m, while within the drift, it extends to around 80 m (Figure 15). From May 7th to May 12th, 2023, a single LHD (FL5) was responsible for removing the ore from the stope during these five days.

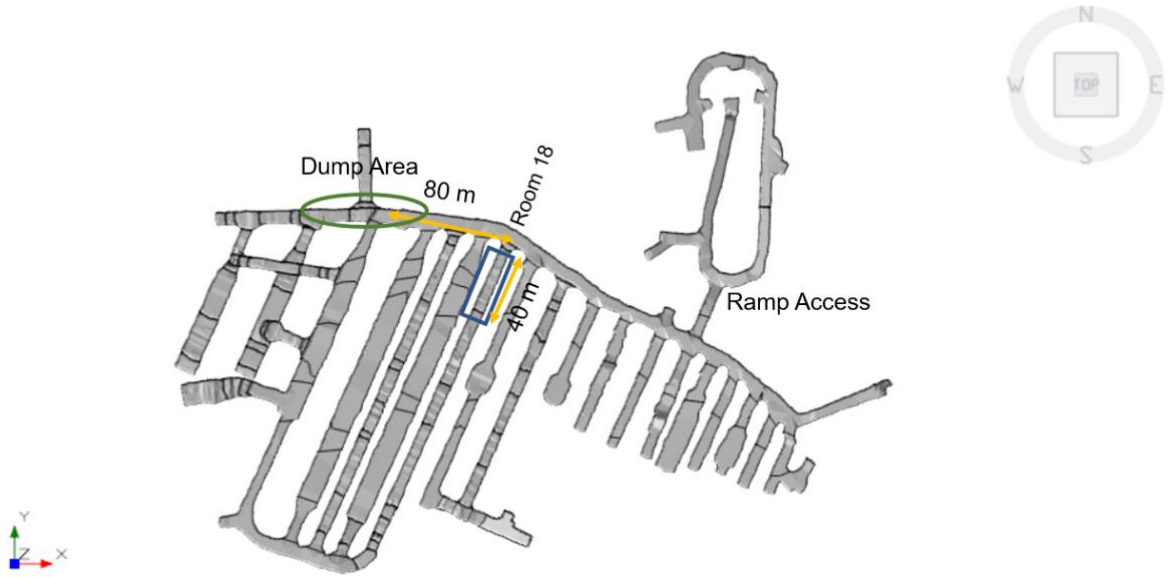

Figure 15: Driving route on level -752 m, remuck bay WC

3.6.3. Long WC Distance

A long WC distance refers to a situation where the loaders' travelling distance is higher than the average distance they typically travel within the underground mine. This occurs when the rooms' location is situated at the end of the drift in the footwall or in the hanging hall, which is on the backside of the stope. In such scenarios, the loaders need to cover longer distances to reach these remote locations, leading to increased travel times and potentially affecting their overall productivity.

On level -1157, stope 13A successfully met all the specified criteria for the Long-Distance work cycle. The average work cycle distance is 720 m long. Within the stope, the average driving

distance is approximately 40 m, while within the drift, it extends to around 320 m (Figure 16). From May 8th to May 17th, 2023, two LHDs (FL2 and FL6) were responsible for removing the ore from the stope during this 9-day period.

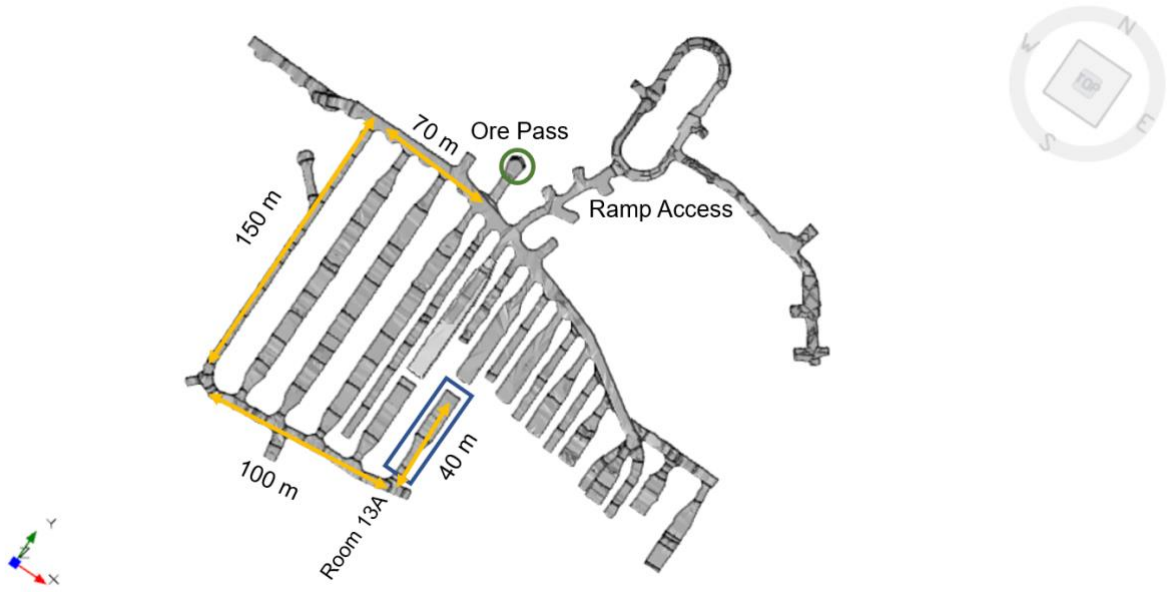

Figure 16: Driving route on level -1157 m, long distance WC

3.6.4. Automate Bucket Fill

In early May, Boliden obtained the "Gold-Version" extension for semi-automated load-haul-dump (LHD) zones from Sandvik. This package introduces several advancements, including the capability for multiple LHD machines to operate simultaneously on the same level and utilise the same ore pass. This is made possible by dividing the level into multiple zones. Additionally, the package enables automated bucket filling, where the machine learns and replicates the operator's behaviour during automated bucket fill operations. As a result, the machine can now complete an entire work cycle independently. The main purpose behind this functionality is to enhance productivity by minimising downtime during lunch breaks.

Levels -1157 and -1257 share similarities in their layout and ore mineralogy, making them suitable for conducting a comparison between automated bucket fill and normal operation. The WC on level 1257 spans 680 m, with 300 m taking place in the drift and 40 m within the stope (Figure 17). During a nine-day period from June 3rd to June 12th, 2023, a single LHD (FL5) was assigned the task of removing the ore from the stope. This specific time frame allows for a focused analysis of the performance and effectiveness of the LHD, providing insights into the potential benefits of automated bucket fill compared to standard operation.

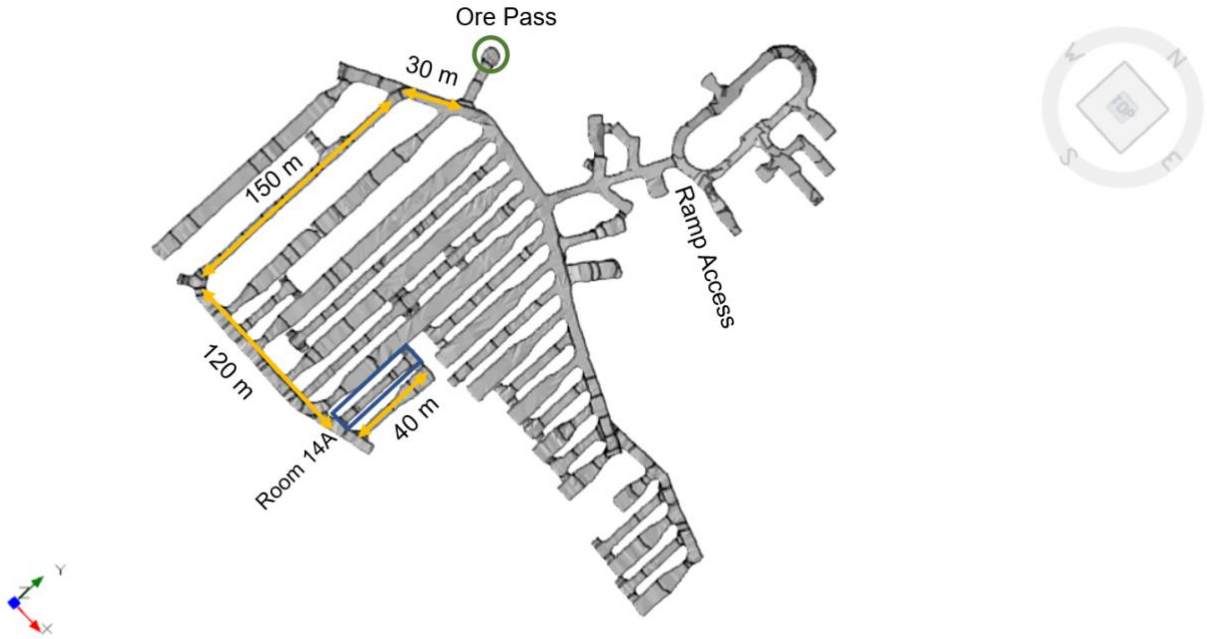

Figure 17: Driving route on level -1257 m, automated bucket fill WC

3.7. Input parameters for the TORO LH518iB VPC Simulations

The following is the input data for the WC simulations of the LH518iB used in the VPC to calculate the performance of the battery loader. A total of 22 simulations were performed to investigate different WCs and ramp distances, dumping methods and sensitivity analyses.

For all base simulations, the following values were used for each WC:

- Bucket Capacity: The bucket capacity for the short WC is set to 15.25 tons, while for the long WC, it is set to 14.9 tons.
- Mucking Time: The time taken by the LH518iB to load the bucket (mucking time) is fixed at 1 min and 30 sec.
- Dumping Time: The time required for the LH518iB to dump the loaded material is set to 30 sec.
- Idle Time: An idle time of 1 minute is added to the simulation to account for overall downtime due to activities such as scanning and loss of connection to the network.

Optimine measures the average bucket fill ratio of the LH621i to be 85% for short WC and 83% for long WC distance. This is then applied to the smaller bucket from the LH518iB. The average mucking and dumping time is calculated to be 1 min and 30 sec and 30 sec, respectively. The 1-minute idle time was added to simulate the overall downtime due to scanning and network connection loss.

3.7.1. WC Distance

Two different distances were selected to analyse the effects of WC distance on machine and battery performance based on the mine layout and LH621i routes.

The shot WC distance, documented in Table 8, spans a total length of 300 m. In order to allow for an extended swapping time window and ensure a minimum running time of three hours for both batteries, the lower SOC limit was changed to 25%.

Whereas the long WC distance, detailed in Table 8, covers a length of 640 m. Consistent with the considerations made for the short WC distance, the lower SOC limit was set to 15% to enable sufficient swapping time and maintain a minimum running time.

Furthermore, both WC distances were calculated considering lower and higher charging bay locations to assess the variations and impacts on productivity and battery performance. This analysis will provide insights into how different charging bay placements affect overall productivity and battery utilisation.

Table 8: WC parameters for the short and long-distance simulation

S {L}-WC							
SEGMENTS #	1	2	3	4	5	6	7
DISTANCE [M]	2500	100 {50}	50 {270}	50 {270}	100 {50)}	2500	100
GRADE [%]	±14.3	0	0	0	0	±14.3	
ELEVATION [M]	±354	0	0	0	0	±354	
SPEED [KM/H]	16.9/29	5 {5}	6 {9}	6 {9}	5 {5}	16.9/29	8
WAYPOINTS	charging	mucking	tramming	dumping	tramming	charging	parking

3.7.2. Dumping Method

A scenario was developed specifically for a remuck bay to investigate the effects of different dumping procedures. The intention is to compare later the differences observed in this simulation with the base scenario. However, it should be noted that the remuck bay simulation is only implemented for a short-distance WC. This is because, in typical operations, the ore is usually temporarily stored in a bay or drift located near the mucked stope.

The distance between the mucking point and the dump point decreases when the ore is stored in a bay or drift, as the available space in these storage areas is typically smaller than the volume of ore in the stope. Consequently, a separate simulation for remucking was developed to assess the impact of this procedure on overall efficiency and productivity (Table 9).

Table 9: WC parameters for the remuck bay simulation

RE-WC							
SEGMENTS #	1	2	3	4	5	6	7
DISTANCE [M]	2500	40	80	80	40	2500	100
GRADE [%]	±14.3	0	0	0	0	±14.3	0
ELEVATION [M]	±354	0	0	0	0	±354	0
SPEED [KM/H]	16.9/29	5	6	6	5	16.9/29	8
WAYPOINTS	charging	mucking	tramming	dumping	tramming	charging	parking

3.7.3. Maximum Ramp Distance

The tipping point, or critical threshold, for the tramming distance between the charging bay and the operational area is currently unknown. To determine this tipping point, maximum ramp distances of 3 800 m have been calculated based on the base scenarios for both short and long WC distances, considering both higher and lower-located charging bays. The objective is to meet the shift and day targets without significantly increasing the required machines (Table 10).

Table 10: WC parameters of the maximum ramp distance simulation

S {L}-WC-MAX							
SEGMENTS #	1	2	3	4	5	6	7
DISTANCE [M]	3800	100 {50}	50 {270}	50 {270}	100 {50}	3800	100
GRADE [%]	±14,3	0	0	0	0	±14,3	0
ELEVATION [M]	±538	0	0	0	0	±538	0
SPEED [KM/H]	16.9/29	5 {5}	7 {9}	7 {9}	5 {5}	16.9/29	8
WAYPOINTS	charging	mucking	tramming	dumping	tramming	charging	parking

3.7.4. Sensitivity Analysis

A sensitivity analysis is conducted to explore the effects on productivity and battery performance by improving the following factors: speed, idle time, mucking and dumping time, and bucket capacity. The improvements were considered at increments of 10%, 15%, and 20% based on data from New Afton, which indicated positive improvements in all these factors (Acuña et al., 2022).

The analysis was performed for both short and long WC distances, taking into account lower and higher-located charging bays. In the sensitivity analysis, only positive improvements were considered (Table 11 and Table 12).

For idle, mucking, and dumping times, the values were reduced to 54 seconds, 51 seconds, and 48 seconds for both short and long WC distances. This decrease in time indicates increased operational efficiency.

Regarding bucket capacity, for the short WC distance, the capacity was increased from the initial 15.25 tons to 16.78 tons, 17.55 tons, and 18 tons as part of the sensitivity analysis. Similarly, for the long WC distance, the bucket capacity was increased from 14.91 tons to 16.5 tons, 17.5 tons, and 18 tons.

Table 11: WC parameters of the short-distance sensitivity analysis 10%, 15% and 20% increase

S-WC 10%(15%) {20%}							
SEGMENTS #	1	2	3	4	5	6	7
DISTANCE [M]	2500	100	50	50	100	2500	100
GRADE [%]	±14,3	0	0	0	0	±14,3	0
ELEVATION [M]	±354	0	0	0	0	±354	0
SPEED [KM/H]	16.9/29	5.5(5.75){6}	6.6(6.9){7.2}	6.6(6.9){7.2}	5.5(5.75){6}	16.9/29	8
WAYPOINTS	charging	mucking	tramming	dumping	tramming	charging	parking

Table 12: WC parameters of the long-distance sensitivity analysis 10%, 15% and 20% increase

L-WC 10%(15%) {20%}							
SEGMENTS #	1	2	3	4	5	6	7
DISTANCE [M]	2500	50	270	270	50	2500	100
GRADE [%]	±14,3	0	0	0	0	±14,3	0
ELEVATION [M]	±354	0	0	0	0	±354	0
SPEED [KM/H]	16.9/29	5.5(5.75){6.6}	9.9(10.4){11}	9.9(10.4){11}	5.5(5.75){6.6}	16,9/29	8
WAYPOINTS	charging	mucking	tramming	dumping	tramming	charging	parking

3.8. Underground Power Grid Capacity

Several companies are currently conducting experiments with various charging methods in the mining industry, such as fast charging, battery swapping, and trolley lines (Leonida, n.d.)(Paraszczak, Laflamme, et al., 2014). However, these methods place additional demands on the mine power grid and strain its capacity (Habib et al., 2018). In the context of underground mining, the availability of electricity is limited and cannot be easily increased (Habib et al., 2018). Boliden recognises this challenge and is exploring a charging approach that involves slower charging over an extended period (The Electric Mine, 2022). This method requires lower voltage, thereby reducing the burden on the power grid. Furthermore, the company has decided to renew and increase its monitoring capabilities (Electrician Engineer, personal communication, May 2023).

For instance, if Boliden aims to charge the battery of an LH518iB within an hour, the required electricity output would be 600V (Electrician Engineer, personal communication, May 2023). However, discussions with Sandvik officials have revealed that fast charging can potentially diminish the battery life. Therefore, it is advisable for Boliden not to pursue fast charging. Additionally, charging the battery within an hour is unnecessary, as a single battery should ideally provide sufficient power for at least 3 to 4 hours. Consequently, charging the battery at one-third or one-fourth of the voltage needed for an hour-long charge would extend the charging time to three hours, but it would still be feasible and suitable (Sandvik, personal communication, 2023).

Boliden has contracted the expertise of ABB, a company responsible for the power infrastructure at the mine site. ABB is assisting Boliden in modernising the power grid, which includes enhanced monitoring of current utilisation and the ability to redirect in time power if necessary. While the data on the power grid's capacity has been inconclusive over the last month due to the ongoing transformation, it can still provide a rough indication of the daily power utilisation. This information enables Boliden to determine when to charge the batteries and estimate the available power capacity in the underground mining environment (ABB, personal communication, April 2023).

4. Results

This chapter presents the results and findings from the input data for availability, utilization, productivity and energy efficiency, which were derived from the scenario and simulation calculations conducted for the LH621i and LH518iB loaders. Furthermore, the chapter presents the results related to the capacity utilisation of the underground power grid and the cost impact difference between the two technologies.

4.1. Key Performance Indicators

The Key Performance Indicators (KPIs) for both loaders are outlined based on the methodology of the machine performance metrics. The following results were calculated using the functions previously explained in section 3.1.

4.1.1. Availability and Utilization

The investigation period under consideration spans from January 1st to June 30th, totalling 4,320 h. To calculate the availability and utilization, the two loaders, FL2 and FL3, were selected based on their reliable data from Planviewer and Optimine.

The lost time is determined to be 900 hours due to the mine being open for operators only 19 h out of 24 h, with the remaining time dedicated to blasting and ventilating activities. Based on Planviewer data, the maintenance time is estimated to be an average of 1,075 h (Table 13).

The refuelling process for diesel loaders, which occurs during day shifts only and takes approximately 40 min, amounts to 119 h. Combining these with the time losses from cleaning sensors, scanning the ore pile, and network disconnections, the total downtime is calculated to be 349 h. The average time allowed to operate is then determined as 1996 hours, obtained by subtracting maintenance, lost time, and downtime from the total time (Table 13).

Table 13 shows the average production time is calculated to be 580 h. By subtracting the average production time from the average time allowed to operate, the machines' average idle time is 1,236 h.

Using Equation 1, the availability is calculated for each LHD, resulting in an average availability of 85%. Equation 2 is to calculate the utilization of availability of each LHD, with an average value of 29%. The MTBF is determined to be 29 h, while the average MTTR is 54 h (Equation 3 Equation 4) (Table 13).

Specific values for the battery loader are unknown and estimated based on literature, data from New Afton, or Boliden's targets. Assuming the same delta time of 4,320 h, the planned maintenance time is estimated to decrease by 55% (Sandvik, personal communication, 2023) due to fewer parts like the gearbox, engine, and hydraulics. The average time loss for swapping from all simulations results in 310 h, as swapping occurs at least once per shift. Similar to the diesel loader, the battery loader is assumed to face the same issues with connection, sensors, etc., resulting in the same time loss (Table 13).

This leads to a total downtime of 540 h, resulting in an allowed operational time of 2,397 hours. Thus, the availability of the battery loader is calculated to be 82%, while Boliden's target for utilization is 66% (Table 13).

Table 13: Results of the availability and utilization

CATEGORY/EQUIPMENT	LHD FL2	LHD FL3	LHD AVERAGE	BLHD
TOTAL TIME [H]	4,320	4 ,20	-	4,320
TOTAL MAINTENANCE TIME [H]	929	1,221	1,075	484
LOST TIME	900	900	900	900
TOTAL TIME LOSS DUE TO REFUELLING/SWAPPING [H]	119	119	119	310
TOTAL TIME LOSS DUE TO SCANNING, LOSS OF CONNECTION, CLEANING [H]	230	230	230	230
DOWN TIME [H]	349	349	349	540
TIME ALLOWED TO OPERATE [H]	2,142	1,850	1,996	2,397
PRODUCTION TIME [H]	592	569	580	1,390
IDLE TIME [H]	1,551	1,281	1,236	1,318
AVAILABILITY [%]	86	84	85	82
UTILIZATION [%]	28	31	29	58
MEAN TIME BETWEEN FAILURES (MTBF) [H]	30	28	29	
MEAN TIME TO REPAIR (MTTR) [H]	46	61	54	

4.1.2. Productivity of the LH621i

The productivity graph depicts time in hours on the X-axis and cumulative tons on the Y-axis. The time interval on the X-axis corresponds to a 9.5-h shift, ranging from 0 to 220 h. The tons on the Y-axis range from 0 to 12,000. The graph presents production trends and mining operation efficiency over time. All four scenarios are plotted on the same graph, with short distances S-WC and Re-WC represented in grey and long distances in blue (Figure 18).

A time study reveals that the average mucking is approximately 1 min and 30 sec, and dumping the ore takes about 30 sec. The data was collected from 50 different WCs.

The Re-WC demonstrates the highest productivity, achieving 12,000 tons in less than six days. The steep incline of its cumulative tonnage curve indicates high productivity, which is further supported by Figure 18 and Table 14, highlighting its highest tonnage output per hour.

Additionally, the downtime in the overall scenario is relatively low as data points are closely clustered (Figure 18), with an average WCT of about 4 min and 9 sec (Table 14). Despite having an average speed of 6.63 km/h, this can be attributed to the short distances and numerous curves in the WC. The scenario has the highest average bucket-fill ratio of 17.88 tons (Table 14).

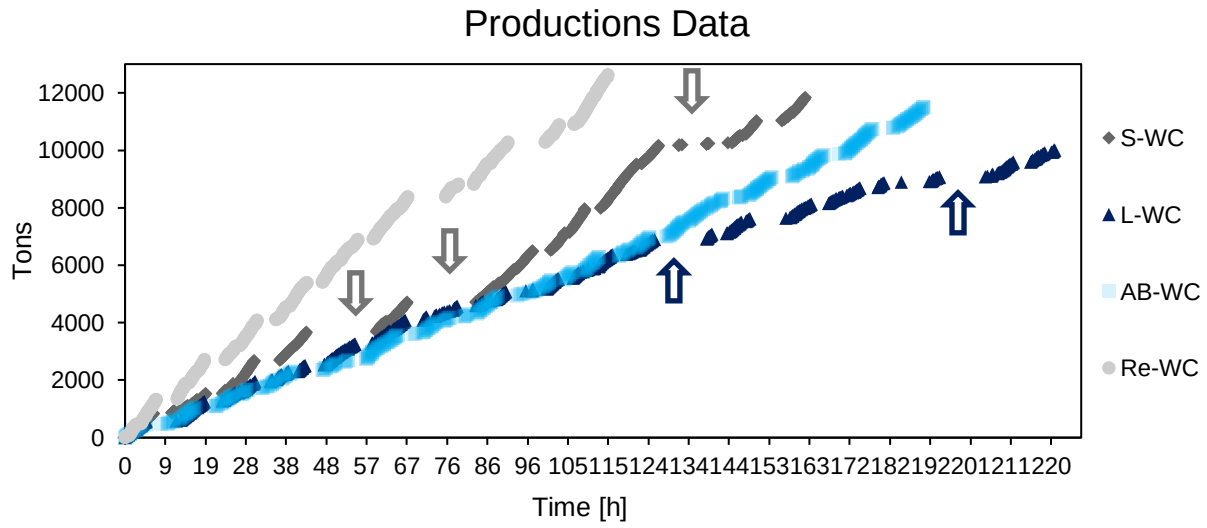

Figure 18: Productivity chart from all scenarios of the LH621i

The AB-WC ranks second in productivity, showing a relatively steady production increase over time without significant disruptions in its productivity curve (Figure 18). Its hourly productivity stands at 80,1 tons per hour, the second-highest among all scenarios. However, it has the lowest bucket fill ratio of 17,34 tons and the second-longest WCT of 7 min and 54 sec, with an average speed of 8,23 km/h (Table 14).

The S-WC, ranking third in productivity, faces challenges with three major production stops (indicated by arrows in Figure 18). Two of these stops resulted from stope and ore pass maintenance, while the third one occurred due to a sensor defect on the LHD, causing production disturbances. The production incline is flatter at the beginning of mucking room 801-23 but increases between hours 80 to 124 before declining towards the end, indicating higher productivity in the middle part and lower productivity at the beginning and end (Figure 18). With an average output of 67,27 tons per hour, it is the second-lowest value among all scenarios. However, it also has the second-highest average bucket fill ratio and the second-shortest WCT and speed of 5 minutes and 37 sec and 5,29 km/h, respectively (Table 14).

The L-WC exhibits the lowest productivity over the time span. Although productivity was initially similar to the AB-WC until the first of two production stops occurred, it encountered challenges thereafter. The first production stop lacks an explanation, while the second one towards the end was related to water management (Figure 18). Ultimately, the L-WC achieved 8,000 tons, but it took more than 220 h to reach this level. With an average productivity of 62,65 tons per hour, it is the lowest among all scenarios. Additionally, the L-WC has the longest WCT of 8 min and 43 sec, with an average speed of about 7.5 km/h (Table 14).

Table 14: Production results of the LH621i scenarios

KPIS/SIMULATION	S-WC	REMUCK	L-WC	AB-WC
AVERAGE TONS PER HOUR	67.27	131.57	62.65	80.1
AVERAGE BUCKET CAPACITY [T]	17.80	17.88	17.55	17.34
AVERAGE SPEED [KM/H]	5.29	6.63	7.50	8.23
WORK CYCLE TIME [MIN:SEC**]**	05:37	04:09	08:43	07:54

The hourly productivity chart presents the average production in tons over the entire working period but on a scale of 24 h. The chart offers insights into the overall production rates and efficiency over an entire day. For each of the scenarios, it is evident that there is no production recorded during the time period from 3 am to 5 am and from 4 pm to 5 pm. This lack of production is due to scheduled blasting activities that occur daily at 4 am and 4 pm. As a safety precaution, all work operations need to be halted during these blasting periods to ensure the well-being of the workers and to comply with safety regulations. Therefore, the absence of production during these time intervals is a result of the necessary suspension of work activities during blasting operations (Figure 19).

Based on the Figure 19, it can be observed that the highest productivity occurs between 11 pm to 2 am, followed by 11 am to 2 pm. Conversely, the lowest production rates are observed at the beginning of the shift. Furthermore, production is also notably lower at 9 am and 9 pm. Overall, the chart highlights the variations in productivity throughout different day times. The highest productivity occurs during late-night and early afternoon shifts, while lower productivity is observed during the initial shift hours and designated break times.

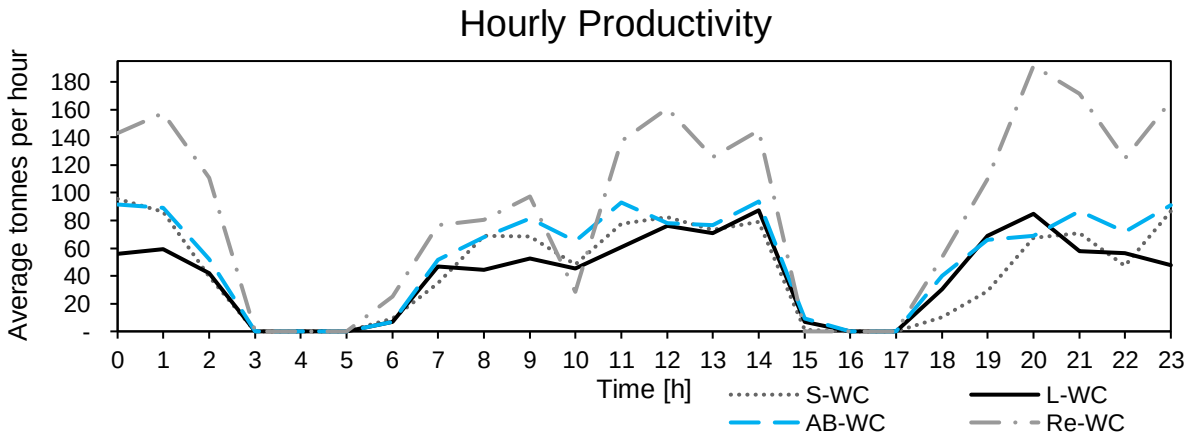

Figure 19: Hourly productivity of the LH621i scenarios

Table 15 summarizes the aggregate shift production for the four scenarios corresponding to 538, 1,053, 501, and 641 tons, whereas the projected maximum production per shift is 1,487, 1,998, 966, and 994 tons. This discrepancy results in performance rates of 0.36, 0.53, 0.52, and 0.64, respectively. These performance rates have direct implications for the OEE values associated with the different work cycle types.

The scenario employing the S-WC exhibits the lowest OEE, with a value of 0.45. In contrast, the RE-WC and the L-WC demonstrate an OEE of 0.54. Finally, the AB-WC achieves the highest OEE value among the scenarios, standing at 0.6 (Table 15).

Table 15: Overall productivity of the LH621i scenarios

	S-WC	RE-WC	L-WC	AB-WC
PRODUCTION PER SHIFT [H]	538	1,053	501	641
POTENTIAL PRODUCTION PER SHIFT [H]	1,487	1,998	966	994
P	0.36	0.53	0.52	0.64
OEE	0.45	0.54	0.54	0.60

4.1.3. Productivity of the LH518iB

In the base simulations, it is initially assumed that the LH621i and LH518iB mining machines have identical values regarding speed, bucket-filling ratio, mucking and dumping capacity because it was impossible to determine these values for Garpenberg without testing the battery loader on site.

Figure 20 illustrates the impact of the WC distance on the SOC and productivity. Both short-range WC simulations, S-WC-LCB and S-WC-HCB, show similar SOC performances. In both simulations, the battery swap takes place after about 240 min, and the shift is completed after approximately 470 min, where the second swap happens. The low-level charging station (LCB) simulation starts with a SOC of 95 %, thus with a fully charged battery. The simulation of the higher charging station (HCB), on the other hand, starts with a SOC of 88%. So the battery does not overcharge when driving downhill. To ensure sufficient charging time for each cycle, the lower SOC threshold is manually set to 25%, which causes the software to initiate the swap earlier. This guarantees a charging availability of at least 3 h, which is essential for slow charging (Figure 20). The average tonnage production per hour for both simulations is 129.63 tonnes, with a cycle time of 06:15 min and an average speed of 5.56 km/h (Table 16).

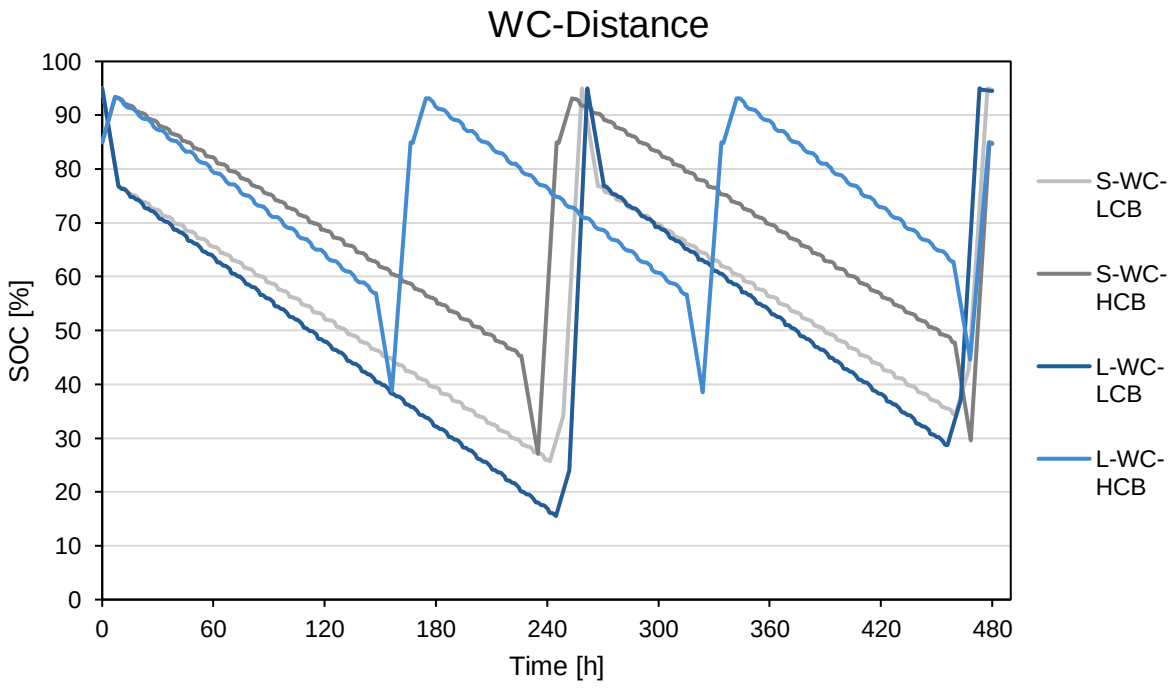

Figure 20: Comparison of the SOC performance on different WC distances and charging bay locations

For the long WC distance simulations, the initial SOCs are the same as for the short WC distance simulation. The L-WC-LCB simulation is almost identical to the short-distance simulation, except for a higher depth of discharge in the first battery stint. Therefore, the lower charge limit is set to 15% to initiate the swap earlier (Figure 20). For the L-WC-HCB simulation, an additional battery swap is required for safety reasons. The machine returns with a SOC of

55% to ensure sufficient battery capacity to reach the next change location. This affects the productivity of the machine and results in an average of 97.81 t/h. The average WCT is extended to 07:48 min, but the average WC speed is 8 km/h (Table 16).

Table 16: Productivity results of the WC distance simulation

	WC DISTANCE SIMULATION	
KPIS/SIMULATION	**S-WC**	**L-WC**
AVERAGE TONS PER HOUR	129.63	97.81
AVERAGE BUCKET FILL RATIO [T]	15.25	14.9
AVERAGE SPEED [KM/H]	5.56	8.00
WORK CYCLE TIME [MIN:SEC**]**	06:15	07:48
VEHICLES REQUIRED FOR DAY TONNAGE TARGET	5	6

Figure 21 depicts the influence of the dumping method on the SOC. The simulation scenarios, S-Re-LCB and S-Re-HCB, are examined. In the S-Re-LCB simulation, the first battery swap occurs after 240 min of production, and the second swap takes place at the end of the shift, with the lower SOC limit set at 15%. On the other hand, the S-Re-HCB simulation involves a first battery swap of around 130 min, a second swap of around 320 min, and a third swap at the shift's end.

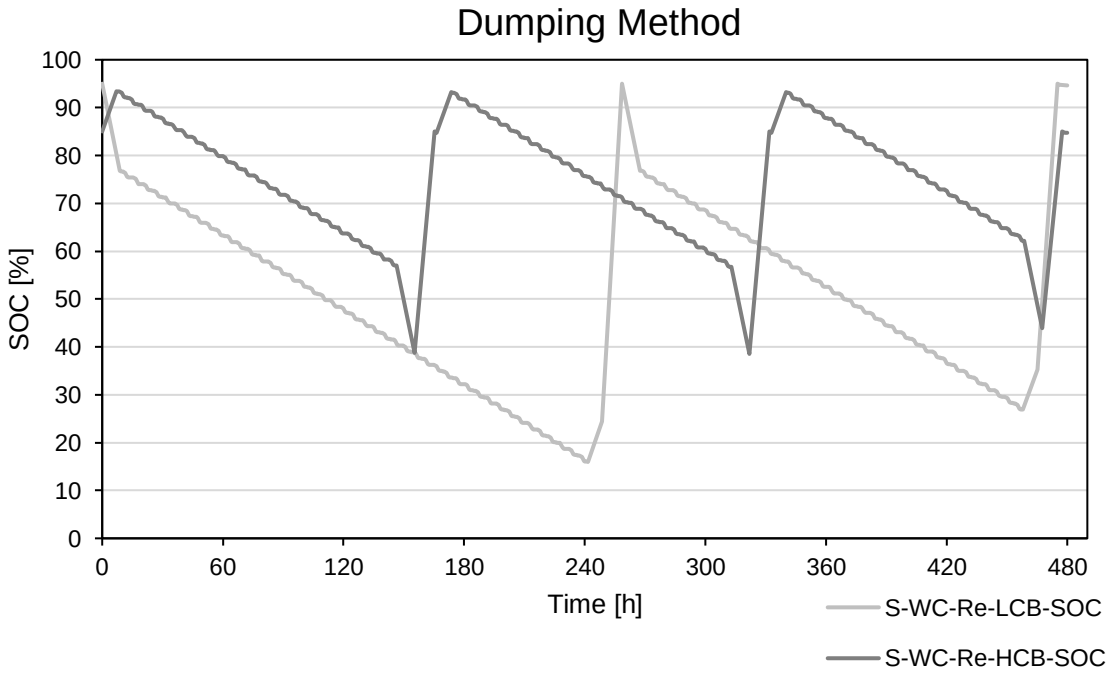

Figure 21: Comparison of the SOC performance impacted by the dumping method and the charging bay location

Both simulations demonstrate high production levels of an average of 151.63 t/h, effectively highlighting the efficacy of the dumping method. The WCT is calculated to be 05:16 minutes, with an average speed of 6.67 km/h (Table 17).

Table 17: Productivity results of the dumping method simulation

KPIS/SIMULATION	Re-WC
AVERAGE TONS PER HOUR	151.63
AVERAGE BUCKET FILL RATIO [T]	15.25
AVERAGE SPEED [KM/H]	6.67
WORK CYCLE TIME [MIN:SEC]	05:16
VEHICLES REQUIRED FOR DAY TONNAGE TARGET	4

In the S-WC-LCB simulation, characterized by a short WC distance and an LCB, the effect on the SOC remains negligible. Battery swaps occur at approximately 230 and 450 min into the shift (Figure 22).

Conversely, the S-WC-HCB simulation with a higher-located charging bay shows a significantly more substantial impact on the SOC. Battery swaps are observed to occur around 150 and 320 min into the shift, indicating a more frequent need for battery exchanges (Figure 22).

In the L-WC-LCB scenario, where the WC distance increases while maintaining the lower charging bay location, the impact on the SOC becomes more pronounced. Battery swaps are initiated earlier, approximately around 200 and 430 min into the shift, leaving only 30 min for productive operation (Figure 22).

In the last simulation, L-WC-HCB, characterized by both an extended WC distance and a higher-located charging bay, the impact on the SOC is further amplified. Multiple battery swaps, totalling four, are necessitated, with swapping intervals observed around 80, 240, 360, and 460 min into the shift (Figure 22).

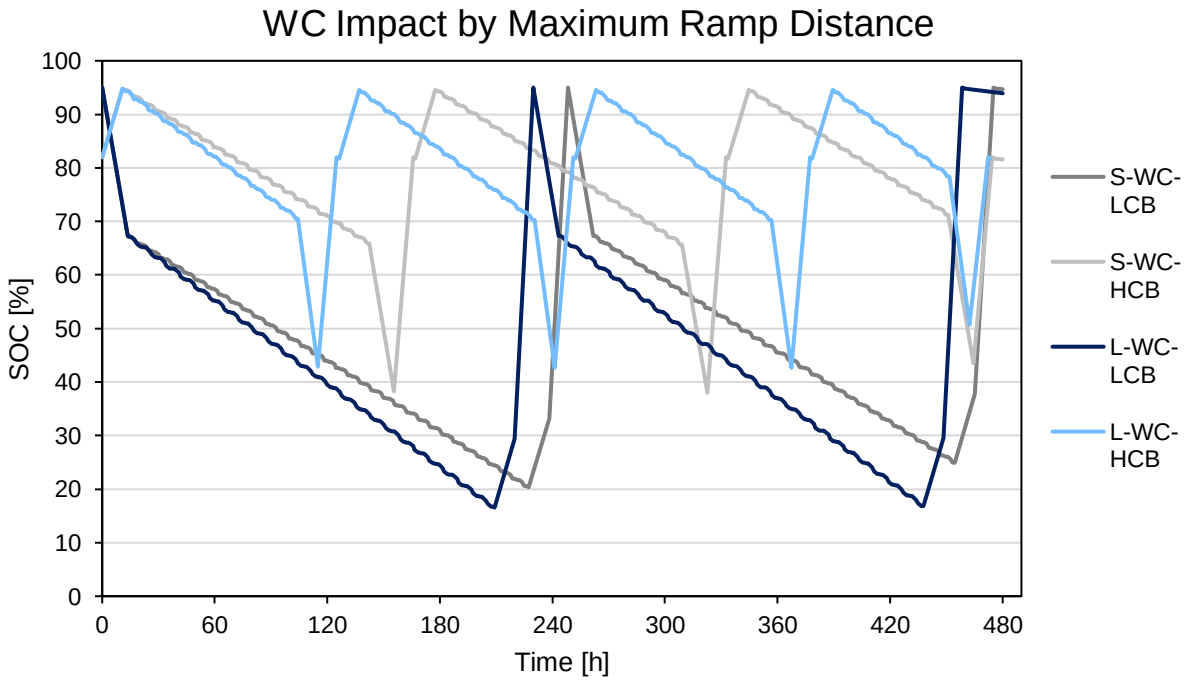

Figure 22: Comparison of the SOC performance with increased ramp distance

These SOC dynamics have a notable effect on productivity, resulting in average production rates of 118.25 and 87.56 tons per hour for S-WC and L-WC, respectively. Since the WC parameters remain the same as in the WC distance simulation, average speed and WCT results remain unchanged (Table 18).

Table 18: Productivity results of the maximum ramp distance simulation

	MAXIMUM RAMP DISTANCE	
KPIS/SIMULATION	**S-WC**	**L-WC**
AVERAGE TONS PER HOUR	118.25	87.56
AVERAGE BUCKET FILL RATIO [T]	15.25	14.9
AVERAGE SPEED [KM/H]	5.56	8.00
WORK CYCLE TIME [MIN:SEC**]**	06:15	07:48
VEHICLES REQUIRED FOR DAY TONNAGE TARGET	5	7

For the purpose of the sensitivity analysis, the values were adjusted as the actual performance data for the Garpenberg mine is not known. Based on the data obtained from New Afton, it could be assumed that a performance improvement can be achieved. Therefore, the values were increased to investigate the potential impact of performance improvement on productivity KPIs like speed, bucket fill ratio, mucking and dumping performance and idle time. This assumption is supported by various research papers, including that of Paraszczak (Paraszczak, Laflamme, et al., 2014) and Sandvik's white paper (Sandvik, personal communication, 2023), as well as practical tests at the New Afton mine(Acuña et al., 2022), which indicate that performance improvement is possible with the battery loader. Hence, these KPIs will be improved by 10%, 15% and 20%.

Table 19 provides a summary of the productivity obtained from a sensitivity analysis of key parameters that affect the overall performance of the loader's operation.

Productivity improvements are observed with varying parameter enhancements for the short WC distance simulation. The average tons per hour increased to 172, 189.75, and 209.25, respectively. The bucket fill ratio also improves, reaching 16.78, 17.55, and 18 tons. The average speed increases from 5.29 km/h to 5.82 km/h, 6.09 km/h, and 6.35 km/h, respectively. Additionally, the WCT decreases to 04:58, 04:46 and 04:33 min Table 19.

In the case of the long WC distance simulation, parameter improvements result in productivity enhancements of 131.19, 141.5, and 154.38 tons per hour, respectively. The average speed per simulation also improves, reaching 8.8, 9.23, and 9.96 km/h. Furthermore, the WCT decreases to 06:25, 06:05 and 05:48 min (Table 19).

Table 19: Productivity comparison of the sensitivity analysis

KPIS/SIMULATION	S-WC+10%	S-WC+15%	S-WC+20%	L-WC+10%	L-WC+15%	L-WC+20%
AVERAGE TONS PER HOUR	172.00	189.75	209.25	131.19	141.50	154.38
BUCKET FILL RATIO [T]	16.78	17.55	18	16.4	17.14	17.9
MUCKING PERFORMANCE [MIN:SEC**]**	01:21	01:16	01:12	01:21	01:16	01:12
DUMPING PERFORMANCE [MIN:SEC**]**	00:27	00:26	00:24	00:27	00:26	00:24
AVERAGE SPEED [KM/H]	5.82	6.09	6.35	8.8	9.23	9.96
WORK CYCLE TIME [MIN:SEC**]**	04:58	04:46	04:33	06:25	06:05	05:48
VEHICLES REQUIRED FOR DAYLY TONNAGE TARGET	4	4	3	5	5	4

The analysis reveals that as performance improves, the workload capacity per battery load increases, leading to the need for earlier battery swaps due to higher energy consumption. However, for most of the LCB simulations, only one battery swap is required, except for the L-WC-LCB+20%, which needs two swaps within the shift time, similar to the HCB simulations. Among the LCB scenarios, the first battery is depleted to the lowest SOC limit of 10%, while the second battery returns with different SOC levels, ranging from 30% (S-WC-LCB+10%) to 11.5% (L-WC-LCB+15%) (Figure 23).

The behaviour for all HCB simulations is similar concerning the lower and upper SOC limits. The only difference is that the time shifts to the left with increasing performance, indicating higher energy consumption and, thus, earlier battery swaps (Figure 23).

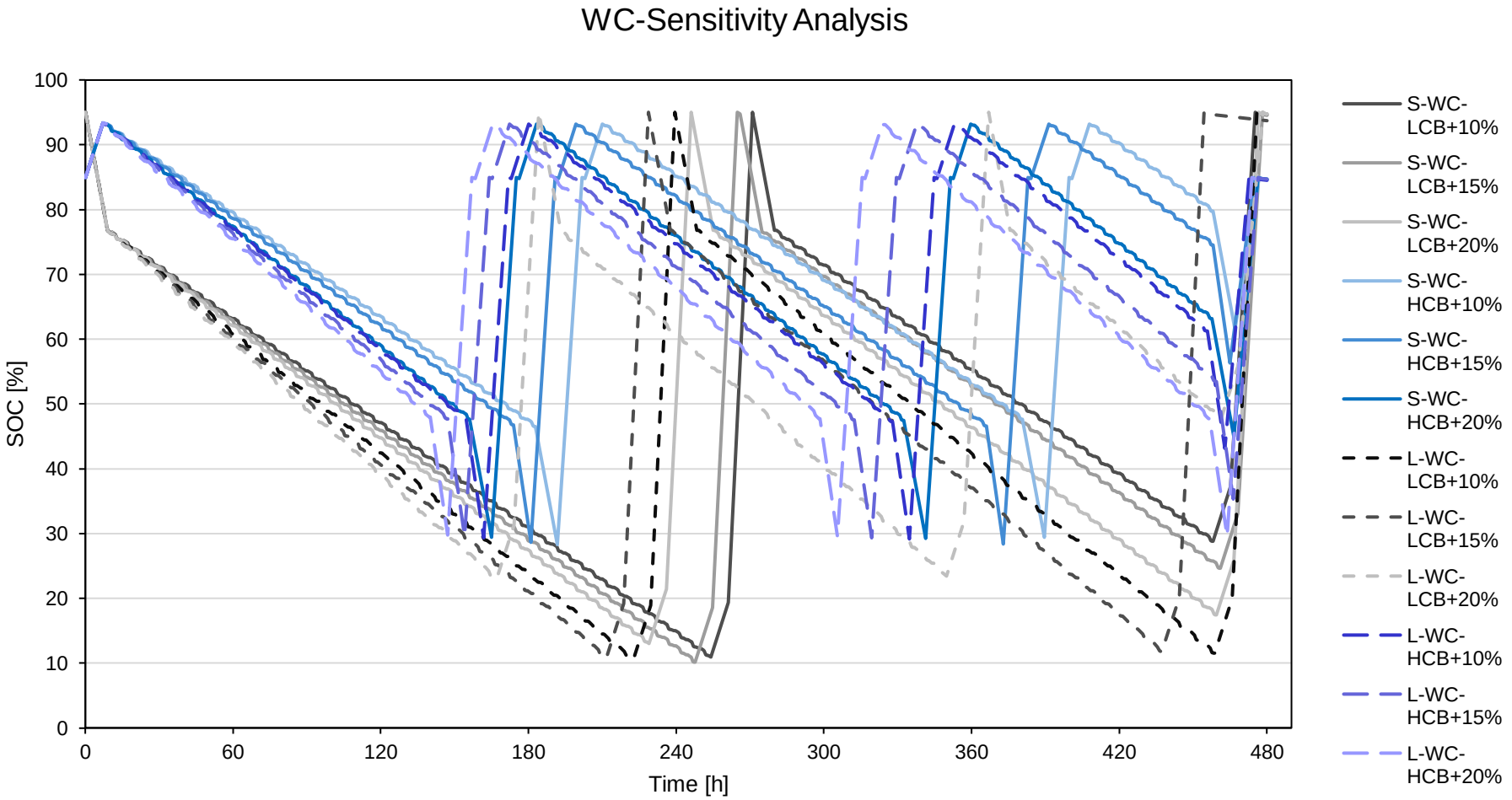

Figure 23: Comparison of the SOC performance in the sensitivity analysis

The total shift production for the base simulations are as follows: 1,037, 783, 1,213, 946, and 701 tons, respectively. The calculation of potential production involved an analysis of idle time for each simulation, which was then divided by the WCT to determine the extra work cycles. These additional cycles were multiplied by the average BFF, and the resulting value was added to the tons per shift to obtain the potential production per shift (Table 20).

Among the various simulations, the highest performance rate and OEE are observed in the L-WC scenario, with values of 0.88 and 0.75, respectively. The second-highest performance rate is found in the S-WC simulation with the same OEE value. The remaining simulations fall between these two extremes in terms of their performance rates and OEE values (Table 20).

Table 20: Production comparison of base simulations

	S-WC	L-WC	RE-WC	S-WC-MAX	L-WC-MAX
PRODUCTION PER SHIFT	1,037	783	1,213	946	701
POTENTIAL PRODUCTION PER SHIFT	1,190	887	1,457	1,114	820
P	0.87	0.88	0.83	0.85	0.85
OEE	0.75	0.75	0.73	0.74	0.74

In the sensitivity analysis, the performance rate values range from 0.89 (S-WC +20%) to 0.92 (L-WC +20%). Interestingly, in the short-distance simulations, there is a decrease in the performance rate as the KPIs improve, going from 0.9 to 0.89. However, the OEE remains at 0.76 (Table 21).

In the long-distance simulation, there is a decline in the performance rate from 0.91 (L-WC +10%) to 0.89 (L-WC +15%), but this trend is followed by an increase to 0.92 (L-WC +20%). This same trend is also mirrored in the OEE values well (Table 21).

Table 21: Production comparison of the sensitivity analysis simulations

	S-WC+10%	S-WC+15%	S-WC+20%	L-WC+10%	L-WC+15%	L-WC+20%
PRODUCTION PER SHIFT	1,376	1,518	1,674	1,050	1,132	1,235
POTENTIAL PRODUCTION PER SHIFT	1,527	1,694	1,872	1,148	1,269	1,342
P	0.90	0.90	0.89	0.91	0.89	0.92
OEE	0.76	0.76	0.76	0.77	0.76	0.77

4.1.4. Energy Efficiency

The WC with the highest energy consumption per ton is the L-WC, with 4.07 kWh/t. This WC also has the longest distance, resulting in approximately 32 loads per shift. The second-highest energy consumption per ton is observed in the AB-WC scenario, with 3.88 kWh/t. In this case, the average load per shift is calculated to be 34 loads. The S-WC scenario has the second-lowest energy consumption per ton, with an energy consumption of 2.84 kWh/t, with an average load per shift of 57 loads. Finally, the Re-WC exhibits the lowest energy consumption per ton, with only 2.21 kWh/t. Additionally, it has the shortest WC distance among all the scenarios. The average downtime per shift due to refuelling is 20 min (Table 22).

Table 22: Energy efficiency comparison of the LH621i scenarios

KPIS/SIMULATION	S-WC	RE-WC	L-WC	AB-WC
ENERGY USAGE (KWH/T)	2.84	2.21	4.07	3.88
AVERAGE REFUEL (MIN)	00:20:00	00:20:00	00:20:00	00:20:00
AVERAGE LOADS PER SHIFT	57	62	32	34

The battery loader simulations demonstrate lower energy consumption, with energy usage per ton ranging from 0.41 kWh/t (S-WC) to 0.83 kWh/t (L-WC-Max) in the base case simulations. The S-WC simulations have the shortest average time of 32 min for the whole swapping process. Conversely, the L-WC-Max simulations require the longest time for battery swapping, taking 1 h and 18 min, resulting in the lowest load per shift count of 62, making it the lowest efficient simulation.

In the sensitivity analysis, a clear trend of improved energy efficiency with increased performance and more loads per shift can be observed. With every 5% increase in performance, the average loads per shift increase by 5 counts for the S-WC simulations. Simultaneously, the energy consumption decreases from 0.38 to 0.35 and eventually to 0.34 kWh/t. The average swapping time for all S-WC simulations is 49 min (Table 23).

For the L-WC simulations, a similar trend is evident, although the difference is smaller. The loads per shift increase from 64 to 66 and 69, while the energy consumption decreases from 0.55 to 0.52 kWh/t and then remains stable. The average swapping time for the first two L-WC simulations is 49 min, while it increases to 1 h and 2 min for the last one (Table 23).

Table 23: Energy efficiency comparison of the LH518iB simulations

	WC DISTANCE		REMUCK BAY	MAXIMUM RAMP DISTANCE		SENSITIVITY ANALYSIS					
KPIS/SIMULATION	**S-WC**	**L-WC**	**Re-WC**	**S-WC-Max**	**L-WC-Max**	**S-WC+10%**	**S-WC+15%**	**S-WC+20%**	**L-WC+10%**	**L-WC+15%**	**L-WC+20%**
ENERGY USAGE [KWH/T]	0.41	0.64	0.41	0.53	0.83	0.38	0.35	0.34	0.55	0.52	0.52
AVERAGE SWAPPING TIME PER SHIFT [HH:MIN**]**	00:32	00:49	00:49	01:01	01:18	00:49	00:49	00:49	00:49	00:49	01:02
AVERAGE LOADS PER SHIFT	68	52	80	62	47	82	87	93	64	66	69

In the scenario with the maximum ramp distance, the battery loader encounters an elevation difference of 538 m with an incline of 14.3 degrees and a ramp distance of 3,800 m. When ascending this distance, the machine consumes 97.787 kW of energy but is able to regenerate 45.133 kW when descending. For the standard distance of 354 m elevation difference and 2500 meters ramp distance, the battery loader requires 65.333 kW for ascent and regenerates 29,743 KW when descending. In order to provide a rule of thumb value, the energy required or gained per 100 meters of elevation difference was calculated. The findings reveal that 18.173 kW is consumed for upward travel, while 8.402 kW is regenerated during downward travel on a 14.3 degrees incline. This means that about 46% of the energy used for travelling the ramp upwards can be regenerated by driving the same way downwards (

Table 24).

Table 24: Energy performance on the ramp with 14,3% inclination

ELEVATION [M]	DOWNWARDS [KW]	UPWARDS [KW]
±538	45.133	97.787
±354	29.743	64.333
±100	8.402	18.173

4.2. Power Grid Capacity

The analysis of the provided dataset, encompassing 100,000 measurements from May 4th to May 10th, 2023, reveals the statistical evaluation of underground electricity consumption patterns. The underground power system has a maximum capacity of 10 KV (kilovolts) and consistently maintains a minimum utilization of 5 KV, ensuring a sufficient power supply. Notably, the grid experiences its lowest utilization of around 5 KV at 2 am and 2 pm. Prior to the commencement of work shifts at 6 am and 6 pm, there is a notable surge in electricity demand, indicating peak utilization. Subsequently, the consumption remains relatively stable within the range of 6 to 8 KV until the approach of shift completion, at which point it decreases below 6 KV once again (Figure 24).

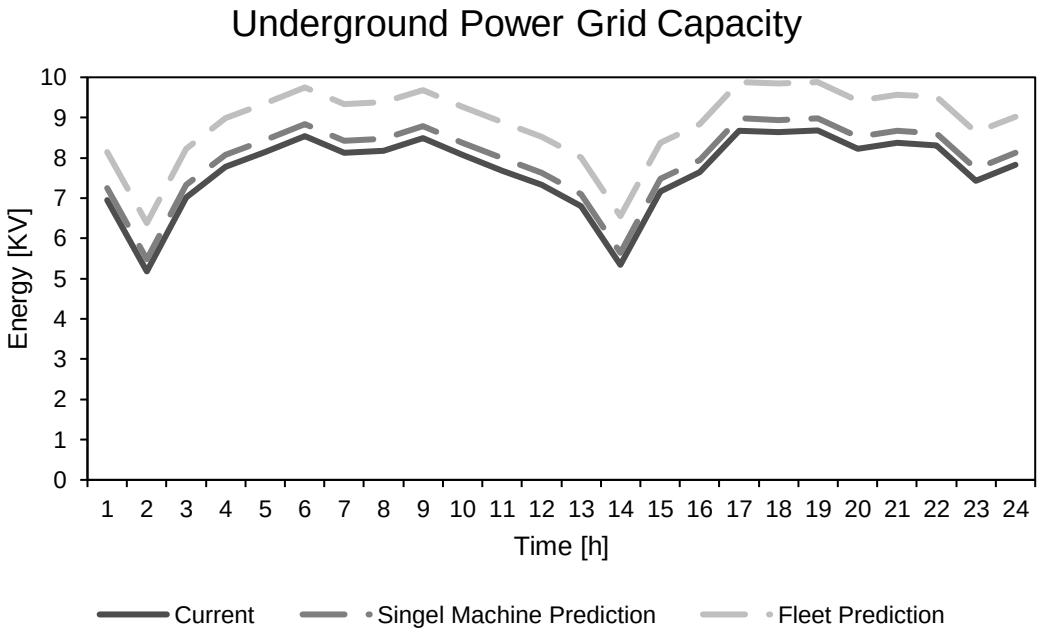

Figure 24: Impact of charging battery loaders on the underground power grid distributed over 24 hours

5. Discussion

In this discussion chapter, the results are analysed, and their relevant implications are explored in detail to highlight their significance in the context of the research objectives. The arguments will be underlined by experienced employees from New Afton, Boliden and Sandvik and also by literature.

5.1. Advantages and Disadvantages of the Simulations

Outlined below are the merits and drawbacks of the scenarios and simulations discussed. Starting of with the scenarios of the LH621i and after that the simulations of the LH518iB.

5.1.1. TORO LH621i

The location of the mining sites, with the different levels having unique ore characteristics that have not been studied before. These differences in rock hardness, mineral content and other factors affect mining productivity. The different total tonnages per scenario can also be seen as problematic, but as more than 9,000 tons were mined in each scenario, it can still be considered conclusive.

However, the use of multiple machines introduces challenges and potential drawbacks. While the utilization of multiple machines for the same stope, it also creates a higher error margin in the collected data. Each sensor has its own inherent error, and when combined with more machines, the cumulative errors can amplify, making it difficult to define the extent of these errors precisely. Furthermore, variations in maintenance levels among the machines can further impact their performance, potentially influencing the accuracy of the collected data.

Another aspect to consider is the potential inaccuracies or misinterpretations that can arise from sensor calibration and signal definition during data collection by Optimine. These factors highlight the importance of conducting statistical evaluations, such as evaluating the WCT, to identify extreme values and mitigate potential errors. By conducting such evaluations, the reliability and accuracy of the collected data can be improved, ensuring its usefulness in decision-making processes.

The limited time window for data collection, spanning from April to June, presents both advantages and disadvantages. On the one hand, it provides actual data about the productivity of LHD machines, allowing for a practical assessment of their performance. On the other hand, the small time frame makes the data sensitive to seasonal fluctuations and other operational complexities. For example, the introduction of summer students, lower utilization of LHDs due to blasting issues, and maintenance complications with new machines and rock falls can all affect productivity and utilization rates, potentially impacting the collected data.

5.1.2. TORO LH518iB

Firstly, the software is unable to accurately simulate fluctuations in the production process, such as breaks, sensor failures, or disconnects to automine (Sandvik USA, personal

communication, May 2023). These unforeseen events can significantly impact the overall efficiency and productivity of the mining operations.

Secondly, the software lacks the capability to calculate acceleration and braking distances. This omission limits the accuracy of the simulation, as these factors play a crucial role in determining the average speed of the machine. Furthermore, the software does not consider curves, which can affect the average speed and further influence productivity and performance (Sandvik USA, personal communication, May 2023).

Another limitation is that the software does not provide the opportunity to differentiate between mucking and dumping times. This means that the time allocated to these processes is assumed based on the LHD scenarios to be the same without accounting for any potential variations or operational considerations that may affect their durations.

However, to simulate potential production losses due to sensor failures, disconnects, or breaks, the idle time in the software was set to one minute in the base cases. This adjustment aims to approximate the potential downtime caused by these events, although it may not fully capture the true impact on productivity.

Considering the maximum speed of 8 to 9 km/h, which is relatively low, it is assumed that the acceleration and braking distances are marginal and can be disregarded. While this assumption simplifies the simulation, it may overlook critical factors that can affect the efficiency of the mining operations.

Furthermore, it is assumed that the smaller dimensions of the BLHD allow for higher speeds in curves, resulting in a higher average speed overall. This assumption is also based on the data from New Afton. Therefore, a more detailed investigation of the curve speed was redundant.

Finally, the fact that mucking and dumping times were not differentiated did not have a significant impact since these times were measured separately before the simulation and then summed to the total value. Therefore, the time for each process is known and can be utilized accordingly.

5.2. Comparison of the TORO LH621i and the TORO LH518iB

This comprehensive comparison enables stakeholders to make informed decisions based on a complete understanding of how each machine performs in various crucial areas. Balancing these factors helps identify the machine that aligns best with the mining operation's goals, whether that be maximizing productivity, reducing environmental impact, or achieving cost savings.

5.2.1. Machine Design

Comparing the LH621i and LH518iB mining machines, characterized by respective bucket volumes of 10.7 m^3 and 8.6 m^3, as well as maximum tramming capacities of 21 tons and 18 tons, the former exhibits superiority. Notably, despite negligible discrepancies of 0.2 seconds in bucket motion times, the LH621i's augmented specifications render it more favourable.

In terms of weight distribution, the LH621i and LH518iB display discrepancies in both unloaded and loaded conditions, with the former being 6.8 tons (unloaded) and 9.8 tons (loaded) heavier, respectively. Remarkably, the front-to-rear axle load ratio is significantly higher for the LH621i (2.6x) than the LH518iB (2.1x) (Sandvik, 2022c and Sandvik, 2020). Line of site observations and insights from operators and Sandvik representatives corroborate the impact of excessive rear axle load on mucking performance, potentially causing rear-end elevation under excessive boom load.

The BLHD equipment exhibits a consistently smaller size compared to the LHD machinery. Specifically, the BLHD's dimensions are reduced by approximately 26% in height, 13% in width, and 6% in length. This reduction in size contributes to a decrease in the turning radius by approximately 6%. Resulting in a turning radius, which has the potential to enhance the equipment's agility, thereby leading to the possibility of achieving higher WC speeds during operational activities (Sandvik, 2022c and Sandvik, 2020).

Delving into propulsion systems, the LH621i boasts a cutting-edge Volvo Stage V diesel engine generating 352 kW, achieving a peak rotational speed of 2,100 rpm. Contrastingly, the LH518iB integrates three electric AC motors, collectively yielding 540 kW and potentially surging to 945 kW at peak performance. This engenders a notable average power advantage of 53% for the electric system over the LH621i's diesel counterpart, escalating further to a peak advantage exceeding 268%. Coupled with the increased rear axle load and enhanced power capabilities, the electric variant is poised to exhibit superior mucking efficiency (Sandvik, 2022c and Sandvik, 2020).

While the effect of the conventional and electric systems on the heat release of the mining environment were briefly discussed, it is important to note that the electric propulsion systems present ancillary benefits that have not been explored in detail in this study. These warrant future comparative investigations due to the reduced heat and diminished DPM emissions associated with electric systems. It is also important to consider the impact of these systems on the mine climate which has been investigated by the Canadian Natural Resources Department at New Afton mine. The results revealed that the electric system maintains a working temperature of 24°C, whereas the conventional system escalates to approximately 56°C. Moreover, the study demonstrates that the conventional system elevates temperature by 3.3°C, whereas the electric system only contributes a minor 0.6°C increment compared to the baseline measurement in the investigated area. While the precise DPM emissions of the LH621i operating in Garpenberg remain uncertain, it is evident that the BLHD eliminates DPM emissions (Lecuyer et al., 2020).

5.2.2. Machine Availability and Utilization

Given the nascent status of battery technology in loaders, the dearth of extended utilization test data underscores the reliance of this thesis on New Afton's experiential insights and Sandvik's theoretical calculations and presumptions. In contrast, the extensive historical use of combustion engines in underground mobile equipment offers a more robust dataset. Nonetheless, a cursory examination of the availability and deployment of two LH621i loaders

at the Garpenberg mine illustrates divergent outcomes across research results and the mine in Garpenberg.

The investigation of these two machines reveals that an availability rate of 85% can be regarded as acceptable in comparison to the 82% calculated with Equation 1. Conversely, the utilization rate of approximately 29% falls short of the 40% utilization rate forecasted by the literature review ((Nieto et al., 2020)). Plausible explanations for this inconsistency can involve suboptimal management of spare parts procurement, evident from instances where the machines were stationed in the service bay for consecutive periods exceeding 20 days. Supply chain issues faced by Boliden and Sandvik, such as the delay in delivering the battery loader by almost a year, can also be considered as crucial factors resulting in a lower utilisation score than predicted. Extreme mechanical damage due to rockfalls or operator mishandling also remains a potential factor. Lastly, the transition of software platforms could have compromised data accuracy, leading to incomplete data entries.

During the same time frame as the LHD investigation, the anticipated additional operational hours for the BLHD stem from Sandvik's projection of a 55% reduction in overall planned maintenance time for the LH518iB compared to conventional LHDs (Toodu, n.d.). However, commensurately, the downtime for the BLHD is anticipated to be lengthened due to frequent battery swaps during shifts, in stark contrast to LHDs' singular daily refuelling requirement. Simulation results underscore the significance of factors such as proximity to charging stations (LCB or HCB), travel distance, and WC distances in dictating the frequency of battery swaps.

Aligning with Boliden's target, the BLHD aims for a utilization rate of 58%. Assuming this target is met, the estimated production time for the BLHD accumulates to 1,390 h, in striking juxtaposition to the average LHD production time of 580 h during the same period.

5.2.3. Machine Productivity

Starting off with the average WC speed in the investigated scenarios. The average speed increases by about 40% between a short and long-distance WC. From observation in the mine, it can be concluded that the speed in the drift is higher because the road is maintained. In the stope itself, the ground is very uneven and therefore, lower speed is required. This means the higher the driving distance in the drift is, the higher the average speed of the WC. In contrast, the amount of curve in the WC impacts the average speed because the curve design is relatively narrow. Again, first-hand monitoring of operators operating the lHD from the automation room shows that the curve speed is reduced to 3 km/h. After applying these speed observations in the simulations, the results are similar to the average WC speeds observed in the scenarios. This leads to the conclusion that the influence of the speed factor should be irrelevant because the average speed is about the same in both scenarios and simulations. Only in the sensitivity analysis the average speed is increased to investigate the impact on the WCT.

The WCT from the S-WC and Re-WC scenarios diverge from the corresponding simulation results by about 10% and 34%. In the case of the L-WC scenario, the deviation to the L-WC simulation is 12%, which the longer distance of the scenario can explain. In comparison, the difference between the AB-WC scenario and the L-WC simulation is only 1%. For each WC in

the simulation, an idle time of 1 min was added to simulate daily delays or failures. This implies that the estimated idle time, the observed speeds and mucking and dumping times party conclude with the scenarios and the simulations. However, the divergence in the short WC distances indicates that the idle time used in the simulation is possibly too high. This can lead to the assumption of a reduced likelihood of delays or failures with decreasing WC distance.

The calculated average bucket fill factor of 0.85 for the S-WC distances and 0.83 for the L-WC distances on LH621i implies that the ore material is very favourable for mucking. This is, however, not always the case because it has been observed that sometimes large rocks many meters wide and high can be found in the well-blasted ore material. It is unclear to Boliden why they are not blasted as planted, but they can lead to much higher WCT by trying to remove them and dragging them into the drift where they are being blasted later. If the LHD cannot remove a block, the work must be put on hold until the block is blasted in the stope.

With an increase in performance of 10%, 15%, and 20% on the base simulation S-WC and L-WC, the sensitivity analysis indicates for the S-WC a production increase of 32%, 46% and 61% and for the L-WC, 34%, 45% and 57%, respectively. The biggest impact on the production improvement is coming from the improved WCT, followed by the BFF. However, it is questionable how much the BLHD can improve in speed and mucking and dumping performances and the objective of road conditions and mine design, but the smaller size and the higher power output should increase the handling, average speed, agility and mucking capabilities (Lecuyer et al., 2020) (Toodu, n.d.).

The OEE corroborates the previously mentioned observations, as depicted in the provided figure and table. The S-WC scenario for the LHD exhibits suboptimal productivity with a factor of 0.45. In contrast, the Re-WC and L-WC scenarios display somewhat improved efficiency, with values of at least 0.54, indicating a reduction in production interruptions during the shift. However, the AB-WC scenario showcases the highest efficiency of 0.6 as production continues during breaks. This assertion is supported by the tonnage curve, which demonstrates a more continuous increase in this scenario compared to the others. Together, the information implies the S-WC scenarios can be seen as inefficient scenarios, marking the lower limit, while the RE-WC is a more efficient and a better example of the average production it is marking the upper limit. The same applies to the long-distance WC scenarios where L-WC marks the lower and AB-WC the upper limit.

The OEE values obtained from the BLHD simulations exhibit a noteworthy trend, with the majority of values exceeding 0.73, indicative of efficient operations. However, it's essential to note that this interpretation holds true for all scenarios except the S-WC simulation, where efficiency is notably lower. These results are explained by the heightened utilization rate and significantly superior performance rate observed in the simulations. Nevertheless, it's important to exercise caution when evaluating these values, as they rely on certain assumptions and, as such, should be interpreted with care (Mousa Mohammadi, Suprakash Gupta, Piyush Rai, 2015).

5.2.4. Machine Energy Efficiency

The efficiency of propulsion systems can be best assessed through their energy utilization efficiency. This metric indicates the proportion of supplied energy that is effectively employed for propelling the vehicle. In the context of normal driving conditions, a combustion engine's efficiency stands at a mere 20%, meaning that more than three-quarters of the energy contained in the fuel is dissipated as waste heat. This substantial loss occurs due to inefficient conversion processes (BMUV, 2021).

In contrast, the electric motor demonstrates a distinct advantage. It converts approximately 80% of the supplied energy into forward motion, exhibiting a significantly higher efficiency rate. Even when accounting for the energy losses incurred during battery charging and electricity supply, the overall efficiency still reaches 64%. Consequently, an electric vehicle (EV) outperforms a conventional internal combustion engine (ICE) vehicle by a factor of three in terms of energy efficiency (BMUV, 2021).

Furthermore, the BLHD possesses the capability to regenerate approximately 46% of the energy it consumes when operating on inclines. This data originates from VPC, although it's important to acknowledge that achieving the same rate of energy regeneration in the specific context of Garpenberg may vary. Cedric De Cauwer investigated the regenerative braking efficiency of EVs and predicted a potential between 15% and 40 % (De Cauwer et al., 2015). Nonetheless, this data provides valuable insight into the potential of the technology and underscores the promising efficiency gains achievable with BLHD technology.

The simulation predicts a remarkable energy efficiency advantage for BLHD technology: it is estimated to be seven times more energy efficient than conventional LHD technology. In addition, the sensitivity analysis shows a promising trend: as tonnage increases and WCT is shortened, energy consumption per ton gradually decreases. This finding underlines the potential for even greater energy efficiency gains with higher productivity and optimized operations (Lecuyer et al., 2020).

5.3. Charging philosophy and power grid capacity

Boliden's long-term plan to transition all mine vehicles from combustion engines to battery-electric vehicles presents challenges related to the simultaneous recharging of the vehicles. If every vehicle needs to be recharged simultaneously, it poses a significant problem. A close investigation into the underground power grid indicates that its capacity is quickly reached during peak periods, specifically from 6 am to 10 am and between 5 pm to 7 pm, when only the loaders are replaced. Therefore, if Boliden intends to switch all vehicles to electric, they must first enhance the capacity of the underground power grid to ensure sufficient energy for recharging the batteries, especially in peak time or find alternative storage capacity.

Alternatively, an option to overcome this challenge is to generate energy within the mine and directly supply it to the battery-operated vehicles. This approach would bypass the need for the entire fleet to rely solely on the existing power grid, providing a potential solution to the simultaneous recharging issue.

However, it is important to note that the data collected on the power grid capacity was only gathered over one week in May. This limited timeframe raises questions about its suitability for creating an accurate yearly prognosis, as seasonal factors like outside temperature can impact ventilation utilization and, consequently, energy consumption. Despite this limitation, it was decided to use the available data to create a prognosis and provide an initial understanding of the potential impacts of battery technology on the underground mining power supply.

Furthermore, recent interviews with Daniel Olsén, who is the head engineer for maintenance and automation in Garpenberg, have revealed that there are currently no plans to increase the regional power grid infrastructure in the near future, which could become problematic. The region's energy demand is projected to rise significantly due to Boliden's proposed expansion of the Garpenberg mine, which aims to double its production. Furthermore, Google is planning to establish a data centre in the Garpenberg region, which will add to the already high energy consumption in the area.

Given the existing power grid infrastructure's limitations and the expected rise in energy demand, tensions may arise between stakeholders regarding the allocation of energy resources in the region.

6. Conclusion

This thesis conducted a comprehensive investigation into different technologies, focusing on performance metrics, availability, utilization, productivity, and energy efficiency. The conventional diesel technology's test scenarios formed the foundation for simulating the battery loader's performance. Utilizing diverse scenarios allowed for establishing both the lower and upper boundaries of the existing production performance achievable with conventional technology.

Employing Sandvik's proprietary VPC software, the simulation of the battery loader revealed its inherent strengths and weaknesses. Notably, due to the substantially higher cost per hour associated with battery technology, the availability of utilization emerged as a pivotal machine performance metric. Moreover, in conjunction with the WC distance, it became evident that the proximity of the charging bay to the mining face significantly influences SOC, thereby impacting performance rate and OEE. The conducted sensitivity analysis demonstrated that augmenting KPIs by 10%, 15%, and 20% translates to remarkable productivity enhancements ranging from 32% to 61%, concurrently bolstering energy efficiency.

It is important to acknowledge that the technology is still in its nascent stages, necessitating time for its full potential to be harnessed and its inherent weaknesses to be mitigated. The necessity for frequent battery swaps during shifts presently limits the technology's flexibility and renders it susceptible to unexpected disruptions. Furthermore, the elevated costs associated with the technology can exert substantial influence on the machine's cost per ton if operational interruptions occur or if planning and scheduling are inadequately executed.

Hence, meticulous planning and a comprehensive understanding of the involved departments are pivotal in maximizing productivity and minimizing the cost per ton. As the technology continues to evolve, careful planning strategies and operational adaptations will be crucial to harness its productivity advantages and to realize its potential as a more efficient and sustainable alternative to conventional technologies.

7. Recommendations

Following the research conducted through this project, some key recommendations for further research and future discussions can be suggested:

1. Enhancing the resilience of the technology against unforeseen incidents and production disruptions can be achieved by upgrading the battery size to 483 kWh. This augmentation not only increases the technology's flexibility but also provides a larger margin for error management for operators and mobile machine schedulers. A larger battery size can better accommodate unexpected interruptions, providing a more reliable and continuous operation.
2. Thoroughly comprehending and investigating the machine's performance under various WC (waiting and charging) distances and charging bay locations will be beneficial. Evaluating the results of such analyses before transitioning the entire fleet to battery loaders can offer valuable insights into optimizing machine performance and minimizing potential disruptions.
3. Dividing the operator group into two teams as part of a strategic approach can minimize lost production time and increase the UoA. This approach enables uninterrupted production during break times. The predictive capabilities of the software can aid in planning battery swaps efficiently. For instance, while the first group commences their break at 10 o'clock, the operator of the BLHD can carry out the battery swap and return to the mining face. Simultaneously, an operator who has completed their break can take over the machine. Subsequently, the second group can commence their break at 10:45 o'clock.

Incorporating these recommendations can contribute to a more resilient and efficiently managed battery loader operation. By embracing larger battery sizes, conducting comprehensive performance assessments, and adopting strategic scheduling practices, the technology's potential can be maximized while minimizing the impact of unforeseen incidents on production.

References

A Review on Electric Vehicles Technologies and Challenge.pdf. (n.d.).

ABB. (2023, April). *WS electrificaton Boliden—ABB* [Personal communication].

Acuña, E., Le, J., Crossingham, D., & Leones, J. (2022). *New Afton Mine Diesel and BEV LHD Field Test: Dust and Heat Contribution*. Natural Resources Canada.

Akimsar, M. (n.d.). *POWER INFRASTRUCTURE SANDVIK LH518B LOADER*. Sandvik.

Bharathan, B., Sasmito, A. P., & Ghoreishi-Madiseh, S. A. (2017). Analysis of energy consumption and carbon footprint from underground haulage with different power sources in typical Canadian mines. *Journal of Cleaner Production*, *166*, 21–31. https://doi.org/10.1016/j.jclepro.2017.07.233

Blinn, H., Persson, J., & Diemunsch, A. (2023). *Power-at-the-end-of-the-tunnel-electrifying-underground-mining*. Sandvik. https://www.rocktechnology.sandvik/en/landing-page/power-at-the-end-of-the-tunnel---electrifying-underground-mining/

BMUV. (2021, October 1). *Mit wenig Energie viele Kilometer zurücklegen*. https://www.bmuv.de/themen/luft-laerm-mobilitaet/verkehr/elektromobilitaet/effizienz-und-kosten

Boliden Annual and Sustainability Report 2022. (2022).

Bołoz, Ł. (2021). Global Trends in the Development of Battery-Powered Underground Mining Machines. *Multidisciplinary Aspects of Production Engineering*, *4*(1), 178–189. https://doi.org/10.2478/mape-2021-0016

Cancino Martínez, C., Fuenzalida, M., & Kamp, C. (2022). Modelling considerations for cave compaction at New Afton Mine. *Caving 2022: Fifth International*

Conference on Block and Sublevel Caving, 573–582. https://doi.org/10.36487/ACG_repo/2205_39

De Cauwer, C., Van Mierlo, J., & Coosemans, T. (2015). Energy Consumption Prediction for Electric Vehicles Based on Real-World Data. *Energies*, *8*(8), 8573–8593. https://doi.org/10.3390/en8088573

Derrien, M. (2022). *Boliden Summary Report Mineral Resources and Mineral Reserves | 2022*. Boliden. https://www.boliden.com/49cfc1/globalassets/operations/exploration/mineral-resources-and-mineral-reserves-pdf/resources-and-reserves-garpenberg-2022-12-31.pdf

Electrician Engineer. (2023, May). *Electricity demand for the charging bay* [Personal communication].

Gamble, C. (2023, April). *Sandvik LH518B experiences* [Personal communication].

Habib, S., Khan, M. M., Abbas, F., Sang, L., Shahid, M. U., & Tang, H. (2018). A Comprehensive Study of Implemented International Standards, Technical Challenges, Impacts and Prospects for Electric Vehicles. *IEEE Access*, *6*, 13866–13890. https://doi.org/10.1109/ACCESS.2018.2812303

Hamrin, Hustrulid, W., & Bullock, R. (2001). *Underground mining methods and applications*. SME Littleton, CO.

Hertwich, E. (2010). *Assessing the environmental impacts of consumption and production: Priority products and materials*. UNEP/Earthprint.

Humphreys, D. (2020). Mining productivity and the fourth industrial revolution. *Mineral Economics*, *33*(1–2), 115–125. https://doi.org/10.1007/s13563-019-00172-9

Jacobs, W., Hodkiewicz, M. R., & Braunl, T. (2015). A Cost–Benefit Analysis of Electric Loaders to Reduce Diesel Emissions in Underground Hard Rock Mines. *IEEE Transactions on Industry Applications*, *51*(3), 2565–2573. https://doi.org/10.1109/TIA.2014.2372046

Kunze, G., Göhring, H., & Jacob, K. (2002). *Baumaschinen: Erdbau- und Tagebaumaschinen* (M. Scheffler, Ed.). Vieweg+Teubner Verlag. https://doi.org/10.1007/978-3-663-09352-7

Lecuyer, N. L., Rennie, D. W., Krutzelmann, H., & Vasquez, L. (2020). *TECHNICAL REPORT ON THE NEW AFTON MINE, BRITISH COLUMBIA, CANADA*. Rock solid resources. https://newafton.newgold.com/wp-content/uploads/2022/04/02-28-2020-New-Gold-New-Afton-NI-43-101-Technical-Report.pdf

Leonida, C. (n.d.). *Battery-electric Vehicles: Brightening the Mining Industry's Future*.

Liu, Y., Zhang, R., Wang, J., & Wang, Y. (2021). Current and future lithium-ion battery manufacturing. *IScience*, *24*(4), 102332. https://doi.org/10.1016/j.isci.2021.102332

Mining Engineer. (2023, April). *Road maintenance* [Personal communication].

Mousa Mohammadi, Suprakash Gupta, Piyush Rai. (2015). Performance Measurement of Mining Equipment. *International Journal of Emerging Technology and Advanced Engineering*.

Nakajima, S. (1988). *Introduction to TPM: Total Productive Maintenance*. Productivity Press. https://books.google.de/books?id=XKc28H3JeUUC

Nieto, A., Schatz, R. S., & Dogruoz, C. (2020). Performance analysis of electric and diesel equipment for battery replacement of tethered LHD vehicles in

underground mining. *Mining Technology*, *129*(1), 22–29. https://doi.org/10.1080/25726668.2020.1720371

Paraszczak, J., Laflamme, M., & Fytas, K. (2014). Electric load-haul-dump machines: Real alternative for diesels? *CIM Journal*, *4*(1).

Paraszczak, J., Svedlund, E., Fytas, K., & Laflamme, M. (2014). Electrification of Loaders and Trucks – A Step Towards More Sustainable Underground Mining. *Renewable Energy and Power Quality Journal*, 81–86. https://doi.org/10.24084/repqj12.240

ROCKTECHNOLOGY.SANDVIK. (n.d.). *OPTIMINE® ANALYTICS*. Sandvik. https://www.rocktechnology.sandvik/de/produkte/automatisierung/optimine-informationsmanagementsystem/optimine-analytics/

Saddler, H. (2012). Bureau of Resources and Energy Economics. *Dissent*, *38*, 26–32.

Samanta, D. B., & Banerjee, S. J. (n.d.). *IMPROVING PRODUCTIVITY OF MINING MACHINERY THROUGH TOTAL PRODUCTIVE MAINTENANCE*.

Sandvik. (2020). *LH518B TECHNICAL SPECIFICATION*. https://www.rocktechnology.sandvik/en/download-center/technical-specifications/underground-loaders-and-trucks/lh518b-technical-specification/#:~:text=Sandvik%20LH518B%20is%20the%20most,m%20x%204%2C5%20m%20tunnel.

Sandvik. (2022a). *BATTERY BAY DESIGN PLANNING*. Sandvik.

Sandvik. (2022b). *SANDVIK BATTERIES BUILT FOR MINING, ENGINEERED FOR SAFETY*. Sandvik.

Sandvik. (2022c). *TORO^{TM} LH621i TECHNICAL SPECIFICATION*. Sandvik. https://www.rocktechnology.sandvik/en/download-center/technical-specifications/underground-loaders-and-trucks/lh621i-technical-specification/

Sandvik. (2023). *SANDVIK LOAD & HAUL BEV BUSINESS CASE INTRO* [Personal communication].

Sandvik USA. (2023, May). *VPC* [Personal communication].

Sijm, J. P. M., Bakker, S. J. A., Harmsen, H. W., Lise, W., & Chen, Y. (2005). *CO2 price dynamics. The implications of EU emissions trading for the price of electricity*. https://inis.iaea.org/search/search.aspx?orig_q=RN:36113036

The Electric Mine. (2022). *Recommended-Practices-for-Battery-Electric-Vehicles-in-Underground-Mining*. GMG. https://gmggroup.org/guidelines-and-publications/https-gmggroup-org-wp-content-uploads-2023-08-2022-06-23_recommended-practices-for-battery-electric-vehicles-in-underground-mining-pdf/

The Operational Definitions and KPIs Sub-Committee. (2020). *A STANDARDIZED TIME CLASSIFICATION FRAMEWORK FOR MOBILE EQUIPMENT IN SURFACE MINING: Operational Definitions, Time Usage Model, and Key Performance Indicators*. GMG. https://gmggroup.org/wp-content/uploads/2020/08/20200713_Time_Classification_Framework-GMG-DAU-v01-r01.pdf

Tiu, G., Jansson, N., Wanhainen, C., Ghorbani, Y., & Lilja, L. (2021). Ore mineralogy and trace element (re)distribution at the metamorphosed Lappberget Zn-Pb-Ag-(Cu-Au) deposit, Garpenberg, Sweden. *Ore Geology Reviews*, *135*, 104223. https://doi.org/10.1016/j.oregeorev.2021.104223

Toodu, E. (n.d.). Sandvik Load & Haul BEV. *Sandvik*.

Appendix

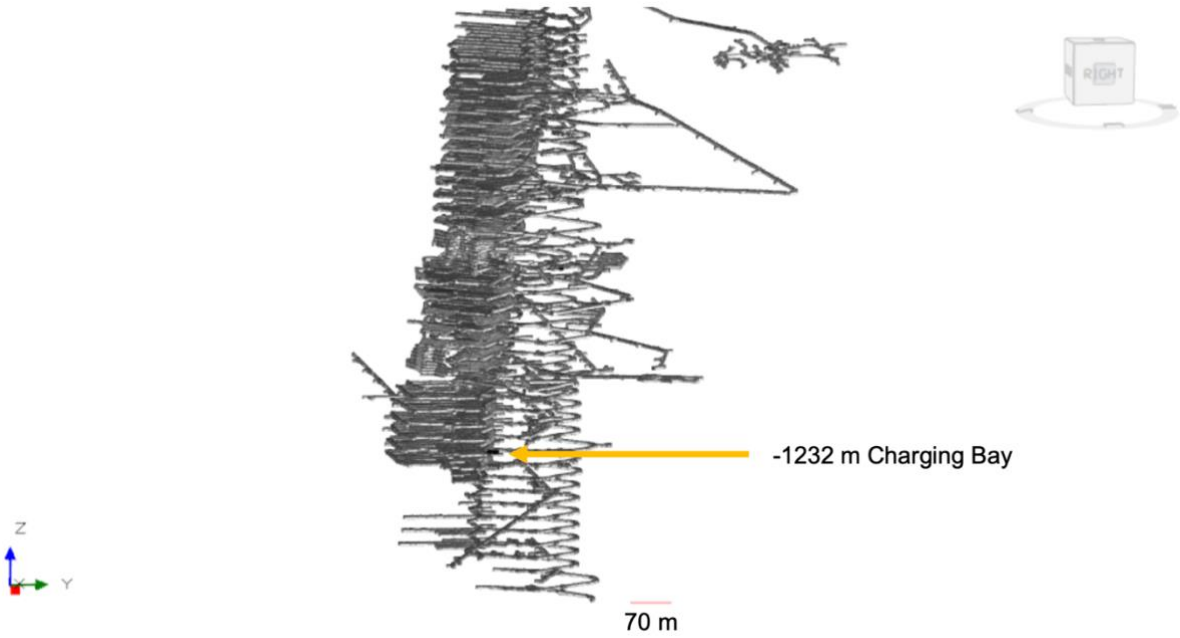

Figure 25: Garpenbergs mine layout

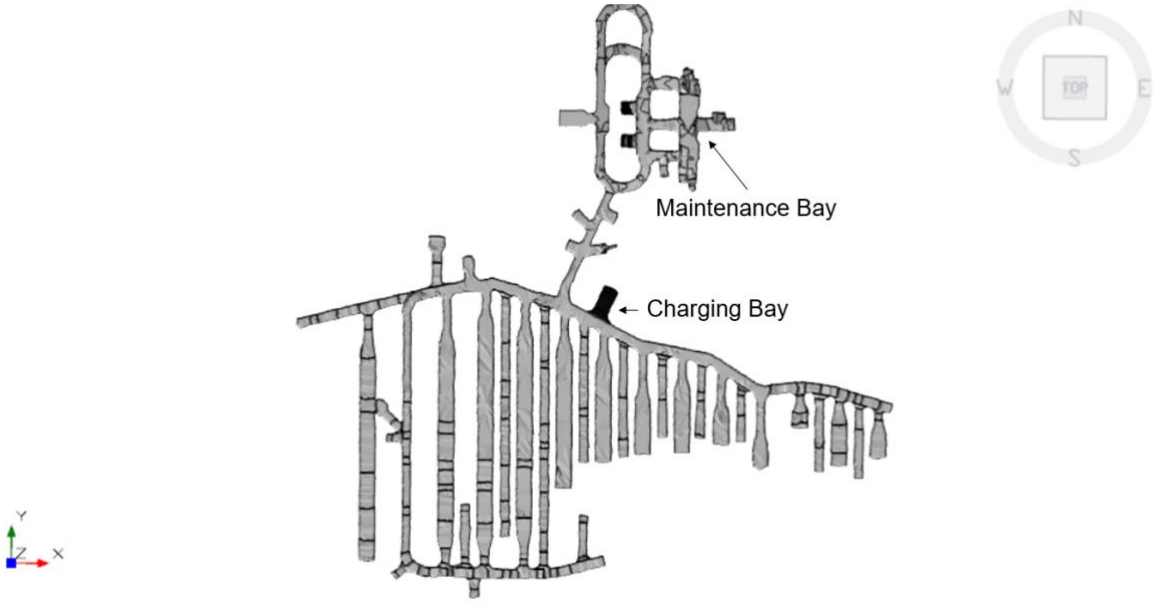

Figure 26: Location of the charging bay and maintenance bay on the level -1232 m

Figure 27: Ore pass entry

Figure 28: Primary Stope -801 m with road condition

Figure 29: Remuck bay

Grade Performance Empty									
Percent grade	0	2	4	6	8	10	12,5	14,3	17
1st gear (km/h)	4,7	4,7	4,6	4,6	4,6	4,6	4,6	4,6	4,5
2nd gear (km/h)	8,4	8,3	8,3	8,2	8,2	8,1	8,1	8	7,4
3rd gear (km/h)	14,6	14,4	14,3	14,1	13,1	11,6	9		
4th gear (km/h)	26,2	25,6	21,3						

Grade Performance Loaded									
Percent grade	0	2	4	6	8	10	12,5	14,3	17
1st gear (km/h)	4,7	4,7	4,6	4,6	4,6	4,6	4,6	4,6	4,5
2nd gear (km/h)	8,4	8,3	8,2	8,2	8,1	7,9	7	6,5	5,7
3rd gear (km/h)	14,5	14,3	14,1	12,1	10,3				
4th gear (km/h)	25,9	21,8							

Figure 30: Grade Performance of the TORO LH621i empty and loaded

Grade Performance															
Percent grade	0	2	3	5	6,7	7,1	7,7	8,3	9,1	10	11,1	12,5	14,3	16,7	20
Speed Loaded (km/h)	27,5	25,2	24	21,7	19,8	19,4	18,8	18,3	17,6	16,9	16	15	14	12,8	11,5
Speed Unloaded (km/h)	28,3	26,6	25,7	23,9	22,5	22,1	21,6	21,2	20,5	19,8	18,9	18	16,9	15,6	14

Figure 31: Grade Performance of the TORO LH518iB empty and loaded

Table 25: 24-hour production table for S-WC

HOUR	SUM PRODUCTION	AVERAGE PRODUCTION
0	948.80	86.25
1	437.43	39.77
2	0	0
3	0	0
4	0	0
5	100.08	9.10
6	382.87	34.81
7	759.00	69.00
8	753.11	68.46
9	529.56	48.14
10	853.04	77.55
11	904.96	82.27
12	806.34	73.30
13	871.38	79.22
14	13.88	1.26

15	0	0
16	0	0
17	112.58	10.23
18	321.51	29.23
19	741.68	67.43
20	779.22	70.84
21	518.77	47.16
22	953.50	86.68
23	1051.74	95.61
TOTAL	11839.45	1,076.31

Table 26: 24-hour production table for Re-WC

HOUR	SUM PRODUCTION	AVERAGE PRODUCTION
0	943.30	157.22
1	664.70	110.78
2	0	0
3	0	0
4	0	0
5	152.10	25.35
6	459.80	76.63
7	484.00	80.67
8	582.60	97.10
9	171.90	28.65
10	822.80	137.13
11	966.10	161.02
12	752.90	125.48
13	870.00	145.00
14	0	0
15	0	0
16	0	0
17	321.60	53.60
18	659.50	109.92
19	1149.30	191.55
20	1028.00	171.33
21	748.50	124.75
22	996.00	166.00

23	857.50	142.92
TOTAL	12630.60	2105.10

Table 27: 24-hour production table for L-WC

HOUR	SUM PRODUCTION	AVERAGE PRODUCTION
0	590.83	59.08
1	419.84	41.98
2	0	0
3	0	0
4	0	0
5	70.46	7.05
6	469.47	46.95
7	445.97	44.60
8	527.39	52.74
9	451.93	45.19
10	605.19	60.52
11	762.49	76.25
12	707.84	70.78
13	873.14	87.31
14	66.52	6.65
15	0	0
16	0	0
17	306.86	30.69
18	689.44	68.94
19	849.64	84.96
20	580.46	58.05
21	566.43	56.64
22	480.03	48.00
23	559.78	55.98
TOTAL	10,023.71	1,002.37

Table 28: 24-hour production table for AB-WC

HOUR	SUM PRODUCTION	AVERAGE PRODUCTION
0	802.3	89.14
1	467	51.89
2	0	0
3	0	0
4	0	0
5	63.1	7.01
6	465.8	51.76
7	612.1	68.01
8	733.7	81.52
9	587	65.22
10	838	93.11
11	704.3	78.26
12	690.3	76.70
13	843.2	93.69
14	83	9.22
15	0	0
16	0	0
17	362.8	40.31
18	595.8	66.20
19	622.1	69.12
20	778.8	86.53
21	644.7	71.63
22	817.7	90.86
23	822.7	91.41
TOTAL	11,534.40	1,281.60

Table 29: Statistical evaluation of the WCT from the S-WC

STATISTICS	VALUE
MIN MIN	3
MAX	9
AVERAGE	5.62
MEDIAN	5
STANDARD	1.30

VARIANZ	1.68
SAMPLE SIZE	607
CONFIDENCE LEVEL	95%
MARGIN OF ERROR	0.103
QUARTILE 1	5
QUARTILE 3	7
INTERQUARTILE RANGE	2
UPPER BOUND	10
LOWER BOUND	2
WCT	00:05:37

Table 30: Statistical evaluation of the WCT from the Re-WC

STATISTICS	VALUE
MIN	3
MAX	6
AVERAGE	4.15
MEDIAN	4
STANDARD	0.92
VARIANZ	0.84
SAMPLE SIZE	379
CONFIDENCE LEVEL	95%
MARGIN OF ERROR	0,092
QUARTILE 1	4
QUARTILE 3	5
INTERQUARTILE RANGE	1
UPPER BOUND	6.5
LOWER BOUND	2.5
WTC	00:04:09

Table 31: Statistical evaluation of the WCT from the L-WC

STATISTICS	VALUE
MIN	4
MAX	12
AVERAGE	8.43
MEDIAN	8
STANDARD	1.36
VARIANZ	1.85
SAMPLE SIZE	460
CONFIDENCE LEVEL	95%
MARGIN OF ERROR	0.124
QUARTILE 1	8
QUARTILE 3	10
INTERQUARTILE RANGE	2
UPPER BOUND	13
LOWER BOUND	3
WCT	00:08:43

Table 32: Statistical evaluation of the WCT from the AB-WC

STATISTICS	VALUE
MIN	5
MAX	11
AVERAGE	7.90
MEDIAN	8
STANDARD	1.20
VARIANZ	1.45
SAMPLE SIZE	377
CONFIDENCE LEVEL	95%
MARGIN OF ERROR	0.121
QUARTILE 1	7
QUARTILE 3	9
INTERQUARTILE RANGE	2

UPPER BOUND	12
LOWER BOUND	4
WTC	00:07:54

Table 33: General information about Garpenbergs mine operations

GENERAL INFORMATION	VALUE LHD	VALUE BLHD	UNIT
EUR2SEK	10	10	SEK/EUR
HOURS PER DAY	24	24	h
SEAT HOURS PER SHIFT	8	8	h
NUMBER OF SHIFTS/DAY	2	2	
DAYS PER YEAR	365	365	
WEEKS PER YEAR	52.14	52.14	
HOURS PER YEAR	8,760	8,760	h
SEAT TIME, HOURS PER YEAR	5,840	5,840	h
SEAT TIME, HOURS PER WEEK	112	112	h
SERVICE TIME PER WEEK	4	3	h
AVAILABLE HOURS PER WEEK	108	109	h
AVAILABLE HOURS PER MONTH	470	474	h
AVAILABLE HOURS PER YEAR	5,631	5,684	h
AVAILABILITY	85%	82%	
UTILIZATION, SEAT TIME	33%	58%	
FUEL CONSUMPTION LHD (2022) [L]	780,640		
CO2 PREIS [SEK]	930		
CO2/LITRE DIESEL	2.68		